Developmental Biology 381 (2013) 241–255

Contents lists available at ScienceDirect

Developmental Biology

journal homepage: www.elsevier.com/locate/developmentalbiology

Embryonic founders of adult muscle stem cells are primed by the determination gene *Mrf4*

Ramkumar Sambasivan [a,1], Glenda Comai [a,2], Isabelle Le Roux [a,2], Danielle Gomès [a], Julie Konge [a], Gérard Dumas [a], Clémire Cimper [b], Shahragim Tajbakhsh [a,*]

[a] Institut Pasteur, Stem Cells & Development, CNRS URA 2578, 25 rue du Dr. Roux, 75724, Paris Cedex 15, France
[b] Institut Pasteur, Department of Developmental & Stem Cell Biology, 25 rue du Dr. Roux, 75724 Paris Cedex 15, France

ARTICLE INFO

Article history:
Received 2 October 2012
Received in revised form
27 March 2013
Accepted 17 April 2013
Available online 25 April 2013

Keywords:
Skeletal muscle stem cells
Mrf4
Myf5
Pax7
Lineage
Reporter mice

ABSTRACT

Skeletal muscle satellite cells play a critical role during muscle growth, homoeostasis and regeneration. Selective induction of the muscle determination genes *Myf5, Myod* and *Mrf4* during prenatal development can potentially impact on the reported functional heterogeneity of adult satellite cells. Accordingly, expression of *Myf5* was reported to diminish the self-renewal potential of the majority of satellite cells. In contrast, virtually all adult satellite cells showed antecedence of *Myod* activity. Here we examine the priming of myogenic cells by *Mrf4* throughout development. Using a Cre-lox based genetic strategy and novel highly sensitive *Pax7* reporter alleles compared to the ubiquitous *Rosa26*-based reporters, we show that all adult satellite cells, independently of their anatomical location or embryonic origin, have been primed for *Mrf4* expression. Given that $Mrf4^{Cre}$ and $Mrf4^{nlacZ}$ are active exclusively in progenitors during embryogenesis, whereas later expression is restricted to differentiated myogenic cells, our findings suggest that adult satellite cells emerge from embryonic founder cells in which the *Mrf4* locus was activated. Therefore, this level of myogenic priming by induction of *Mrf4*, does not compromise the potential of the founder cells to assume an upstream muscle stem cell state. We propose that embryonic myogenic cells and the majority of adult muscle stem cells form a lineage continuum.

Introduction

Vertebrate skeletal muscle development involves the allocation of founder stem cells to the muscle lineage, proliferation of committed myoblasts and subsequently differentiation and fusion of myoblasts to generate multinucleated, contractile myofibres (Biressi et al., 2007a; Sambasivan and Tajbakhsh, 2007). A subset of the myogenic cell pool called satellite cells (Mauro, 1961) remains undifferentiated and associated with myofibres, contributing to repair of the tissue following injury. Cells that fit this anatomical description arise during late foetal stages in chick and mouse, contribute to prenatal and postnatal muscle growth and enter mitotic quiescence in young adults (Gros et al., 2005; Kassar-Duchossoy et al., 2005; Relaix et al., 2005; Relaix and Zammit, 2012). The origin of satellite cells in trunk and limb musculature has been traced to somites, transient epithelial metameric segments of paraxial mesoderm (Armand et al., 1983; Gros et al., 2005; Sambasivan et al., 2011), whereas head muscle satellite cells originate from cranial mesoderm (Harel et al., 2009; Sambasivan et al., 2009). Although much information is available on the genetic regulation of skeletal muscle, as for virtually all organs and tissues, the link between emerging populations of muscle stem cells in the embryo and those in the adult remains largely undefined.

Founder stem cells in the trunk and limb muscle reside in the dorsal epithelial layer of somites called the dermomyotome, and they express the paired-box/homeodomain transcription factors *Pax3* and/or *Pax7*. Notably, *Pax7* expression identifies these cells throughout development starting from early embryogenesis, and it marks all adult satellite cells. The acquisition of myogenic cell fate and lineage progression to myoblasts and differentiated myofibres is directed by bHLH transcription factors known as muscle regulatory factors (MRFs). *Myf5*, *Myod* and *Mrf4* determine muscle identity (Kassar-Duchossoy et al., 2005; Rudnicki et al., 1993), whereas *Myod*, *Mrf4* and *Myogenin* (*Myog*) function to activate or maintain the differentiation programme (Hasty et al., 1993; Nabeshima et al., 1993; Rawls et al., 1995). Embryonic muscle progenitor cells have been categorised into *Myf5*-expressing and *Myf5*-negative (*Myod*-expressing) subpopulations (Braun and Arnold, 1994; Gensch et al., 2008; Haldar et al., 2008). Remarkably,

* Corresponding author. Fax: 33 1 45 68 89 63.
E-mail addresses: shaht@pasteur.fr, shahragim.tajbakhsh@pasteur.fr (S. Tajbakhsh).
[1] Present address: Institute for Stem Cell Biology and Regenerative Medicine, National Centre for Biological Sciences, GKVK, Bellary Road, Bangalore 560065, India.
[2] Equal contributing authors.

0012-1606/$ - see front matter © 2013 Elsevier Inc. All rights reserved.
http://dx.doi.org/10.1016/j.ydbio.2013.04.018

the minority Myf5^{-}Myod^{+} population was reported to expand following the genetic ablation of *Myf5*-expressing cells using diphtheria toxin, thereby rescuing muscle development (Gensch et al., 2008; Haldar et al., 2008). *Mrf4* expression is confined to embryonic progenitors and thus fails to drive myogenesis autonomously beyond the embryonic period in mice lacking *Myf5* and *Myod* (embryonic day E14.5; (Kassar-Duchossoy et al., 2004)). However, it is the most abundant MRF to be expressed in differentiated myonuclei (Hinterberger et al., 1991). Whereas Myod is key to initiate muscle differentiation (see (Berkes and Tapscott, 2005)), Mrf4 plays a role in later phases of differentiation and maintenance of the differentiated state (Zhang et al., 1995). This is highlighted by the absence of myogenesis in *Myod:Mrf4* double null mice (Rawls et al., 1998), where these genes were proposed to be necessary for *Myog* activation in muscle progenitor cells (Kassar-Duchossoy et al., 2004).

In this context, a key question concerns the regulatory state of the founders of adult satellite cells in relation to the relative roles of the MRFs. It is unclear whether satellite cells arise from an 'upstream' Pax^{+}/MRF^{-} population or if they emerge from a committed pool of MRF^{+} progenitors that subsequently revert to a more uncommitted cell state. Firstly, the majority of satellite cells (~90%) were reported to express the *Myf5^{nlacZ}* reporter (Beauchamp et al., 2000; Tajbakhsh et al., 1996a) and also Myf5 protein (Gayraud-Morel et al., 2012). Secondly, using *Myf5^{Cre}:R26^{YFP}* mice it was reported that a small subset of the adult satellite cell pool had never activated *Myf5* and are therefore upstream in the lineage (Kuang et al., 2007). In contrast, the use of

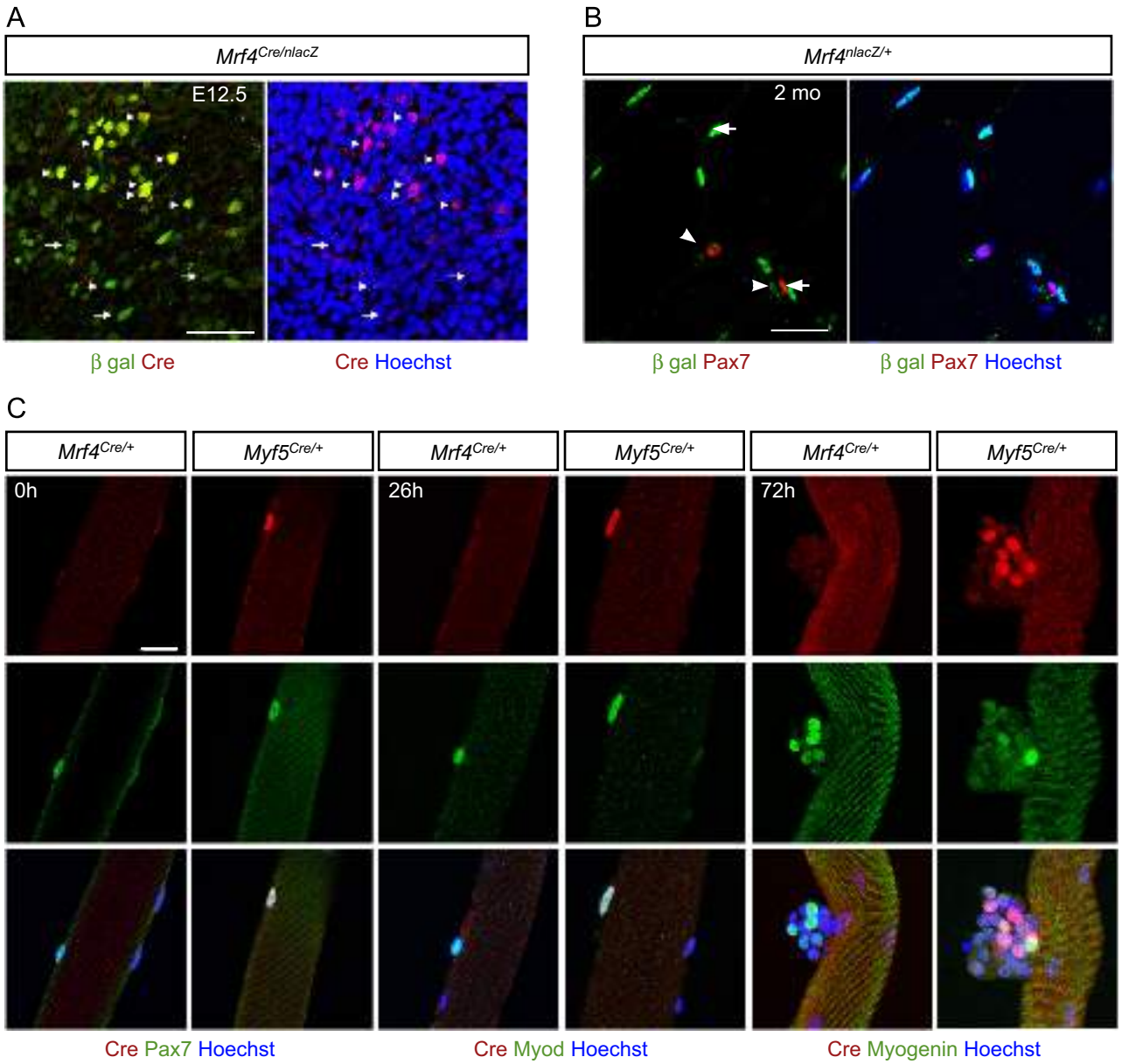

Fig. 1. Cre expression driven by the *Mrf4^{Cre}* allele matches endogenous Mrf4 expression. (A) Immunostained transverse sections of the trunk at forelimb level showing a portion of myotome of an E12.5 embryo. Cre recombinase protein is present in β-gal positive nuclei (arrowheads) but never in β-gal negative cells. β-gal^{+} Cre^{-} cells (arrows) reflect the longer stability of β-gal protein with respect to Cre. (B) TA cross-section of 2 months old (2 mo) mice, immunostained, reveals exclusive staining for Pax7 in satellite cells (arrowheads) and β-gal (*Mrf4^{nlacZ}*) in differentiated myonuclei (arrows). No contemporary expression of Mrf4 in seen in satellite cells in adult mice. (C) EDL fibres from adult (6–8 week old) *Mrf4^{Cre}* or *Myf5^{Cre}* mice were either fixed immediately following isolation (0 h) or after 26 or 72 h in culture. Cre immunostaining in *Myf5^{Cre}* mice co-localised with Pax7 protein at 0 h, with MyoD upon satellite cell activation (26 h) and with Myog during differentiation (72 h). Cre expression from the *Mrf4^{Cre}* allele was not observed in satellite cells at any stage. Scale bars in A, B, C=25 μ.

Myod^{Cre} showed an antecedence of *Myod* activity in virtually all satellite cells (Kanisicak et al., 2009). Although Cre expression does not necessarily report for the presence of a functional gene product from the driver locus (*Myf5* or *Myod*), this result shows that the locus is transcriptionally active indicating a transition in the regulatory cell state. In the present study, we refer to 'priming' as an active *Mrf* locus whereas 'commitment' implies functional MRF protein. Thus, *Myod* primed cells would need to revert to a stem cell state for a satellite cell pool to be set aside in the adult. Taken together, it is unclear whether muscle stem/progenitors transit through regulatory states strictly uni-directionally during lineage progression or if a subset of the ancestral satellite cell pool is derived from uncommitted founder cells.

As *Mrf4* plays a dual role as a determination and differentiation gene, we reasoned that addressing the history of *Mrf4* activity in satellite cells would clarify this issue with respect to the regulatory state of the founders of satellite cells. Furthermore, skeletal muscle development occurs in successive and distinct waves. Although transcriptome analysis and genetic studies have shown that the myoblasts contributing to these temporally defined phases are distinct (Biressi et al., 2007b; Hutcheson et al., 2009; Tajbakhsh, 2009), little is known about the upstream population that assures myogenesis throughout development. In addition, the postnatal phase is distinguishable, at the molecular level, from embryonic and foetal myogenesis (Lepper et al., 2009). The molecular switch from embryonic myogenesis to the foetal muscle programme is at least partly controlled by Nfix (Nuclear factor I/X), resulting in down regulation of embryonic myogenic markers such as slow myosin heavy chain (MyHc) and up regulation of foetal muscle markers such as muscle creatine kinase (*Ckm*), β-enolase (*Eno3*), protein kinase θ (*Prkcq*) (Biressi et al., 2007b; Messina et al., 2010). However, the lineage relationship among these various developmental progenitors and the emerging satellite cells is poorly understood.

Using Cre-lox lineage tracing strategies we report the unexpected finding that virtually all adult satellite cells, independently of their anatomical location or embryonic origin, had transited through a developmental stage in which the *Mrf4* locus was active. We also show that the activation of *Mrf4* in this population commences and is likely to be nearly complete in the embryonic phase. Surprisingly, almost all Pax7^{+} embryonic muscle stem/progenitors in various muscle anlagen induce *Mrf4*. We propose that the various developmental stem/progenitors are linearly related and that the embryonic priming by *Mrfs* does not compromise the 'stemness' of future satellite cells.

Results

Mrf4^{Cre} *activity reflects that of the endogenous Mrf4 locus*

To investigate the priming of stem/progenitors cells by *Mrf4* during the distinct waves of myogenesis, we adopted a Cre-lox genetic strategy, similar to that of previous reports (Kanisicak et al., 2009; Kuang et al., 2007), using *Mrf4*^{Cre} (Keller et al., 2004b). First, we verified that *Cre* expression in *Mrf4*^{Cre} mice truly reflects the activation of the *Mrf4* locus. In the somites of the embryo, *Mrf4* expression precedes or is induced concomitantly with that of *Myf5* (Kassar-Duchossoy et al., 2004). In the absence of reliable antibodies against Mrf4, we compared *Mrf4*^{Cre} expression to another knock-in allele, *Mrf4*^{nlacZ} (*Myf5*^{loxP}: *Mrf4*^{nlacZ}, (Kassar-Duchossoy et al., 2004)). Notably, the genetic modifications in these two alleles are targeted at different sites. In *Mrf4*^{Cre}, *IRES-Cre* is inserted in the 3' UTR of the gene, whereas the *Mrf4*^{nlacZ} involves genetic inactivation of *Mrf4* with the *nlacZ* reporter positioned in the first exon. We analysed *Mrf4*$^{Cre/nlacZ}$ compound heterozygous embryos at embryonic day E12.5 for correspondence of *Cre* expression to that of β-gal (Fig. 1A). We detected Cre recombinase protein only in β-gal^{+} nuclei and never in β-gal^{-} nuclei (100% of Cre^{+} nuclei were β-gal^{+}, whereas 78.7% ± 1.6 of β-gal^{+} nuclei were Cre^{+}; $n=3$ embryos, 192 nuclei). This indicates that β-gal is more stable than Cre protein and that *Mrf4*^{Cre} is a reliable reporter of *Mrf4* activation under these conditions. This result is in agreement with the embryonic role of Mrf4 as a determination factor, as well as genetic studies showing that Mrf4 can autonomously drive embryonic muscle cell fate in the absence of Myf5 and Myod (Kassar-Duchossoy et al., 2004). At post-natal day 21, when Mrf4 functions as a differentiation factor, Cre expressing cells were shown to co-express Myod but not Pax7 (Keller et al., 2004a).

We next assessed Cre expression from the *Mrf4* locus in adult muscle. Mrf4 is the predominant MRF expressed in differentiated skeletal muscle nuclei in mouse (Hinterberger et al., 1991) and as shown in Fig. 1B it is not expressed in adult satellite cells ($n=3$ animals, total of 428 nuclei; see also (Gayraud-Morel et al., 2007)). Following myofibre isolation and in vitro culture, lineage progression from satellite cell quiescence to differentiation can be followed with specific markers (Gayraud-Morel et al., 2007). Using this model, we isolated *Extensor Digitorum Longus* (EDL) muscle fibres from 6 to 8 week old *Mrf4*^{Cre} mice and performed immunohistochemistry immediately following isolation (0 h), after 26 h and 72 h in culture. Fibres isolated from *Myf5*^{Cre} mice (Haldar et al., 2008) were used as positive controls, as *Myf5* is active in the majority of quiescent, and all activated satellite cells (Gayraud-Morel et al., 2012). Cre expression in cells on *Myf5*^{Cre} fibres overlapped as expected, with Pax7-expressing cells in the quiescent state (0 h) and with Myod and Myog expressing cells upon activation and differentiation in culture (at 26 h and 72 h, respectively; Fig. 1C). In marked contrast, Cre expression in *Mrf4*^{Cre} mice was not observed at any stage (Fig. 1C). However, when cells were isolated enzymatically from an injured *Mrf4*^{Cre} *Tibialis anterior* (TA) muscle and allowed to differentiate in vitro, Cre expression was observed in myonuclei of newly formed multinucleated myotubes (Fig. S1). This observation confirms previous observations using the *Mrf4*^{nlacZ} allele (Gayraud-Morel et al., 2007).

Therefore, these results demonstrate that Cre protein is appropriately expressed from the *Mrf4* locus in muscle progenitors during myogenesis and muscle homoeostasis, and notably that Cre is absent from adult quiescent and activated satellite cells.

Pax7 reporter lines increase sensitivity for tracking cells within muscle lineage

We then determined *Mrf4*^{Cre} activity using reporter alleles. First, we analysed *Mrf4*^{Cre}*: R26R*^{lacZ} (Keller et al., 2004b) embryos following whole mount X-gal staining. Surprisingly, comparison between the readout of *Mrf4*^{Cre} expression from *R26R*^{lacZ} reporter (historical/cumulative expression) constituted only a subset of expression detected with the *Mrf4*^{nlacZ} allele (contemporary expression) (Fig. 2A, B). Given that readouts from reporter lines have been shown to impact directly on the interpretation of the outcome of lineage analyses (Ma et al., 2008; Stanley et al., 2002), we reasoned that a lineage specific reporter mouse would increase the resolution for these studies. Pax7 constantly marks muscle stem/progenitors cells from embryonic stages to postnatal life, regardless of the anatomical muscle location (Gros et al., 2005; Kassar-Duchossoy et al., 2005; Relaix et al., 2005; Seale et al., 2000). Thus, the *Pax7* locus is an ideal target for developing reporters to follow the skeletal muscle stem/progenitor population from the embryo to the adult.

We generated two conditional reporter lines at the *Pax7* locus by targeting transgene cassettes into the first exon by homologous recombination. These were designed to express, from the *Pax7*

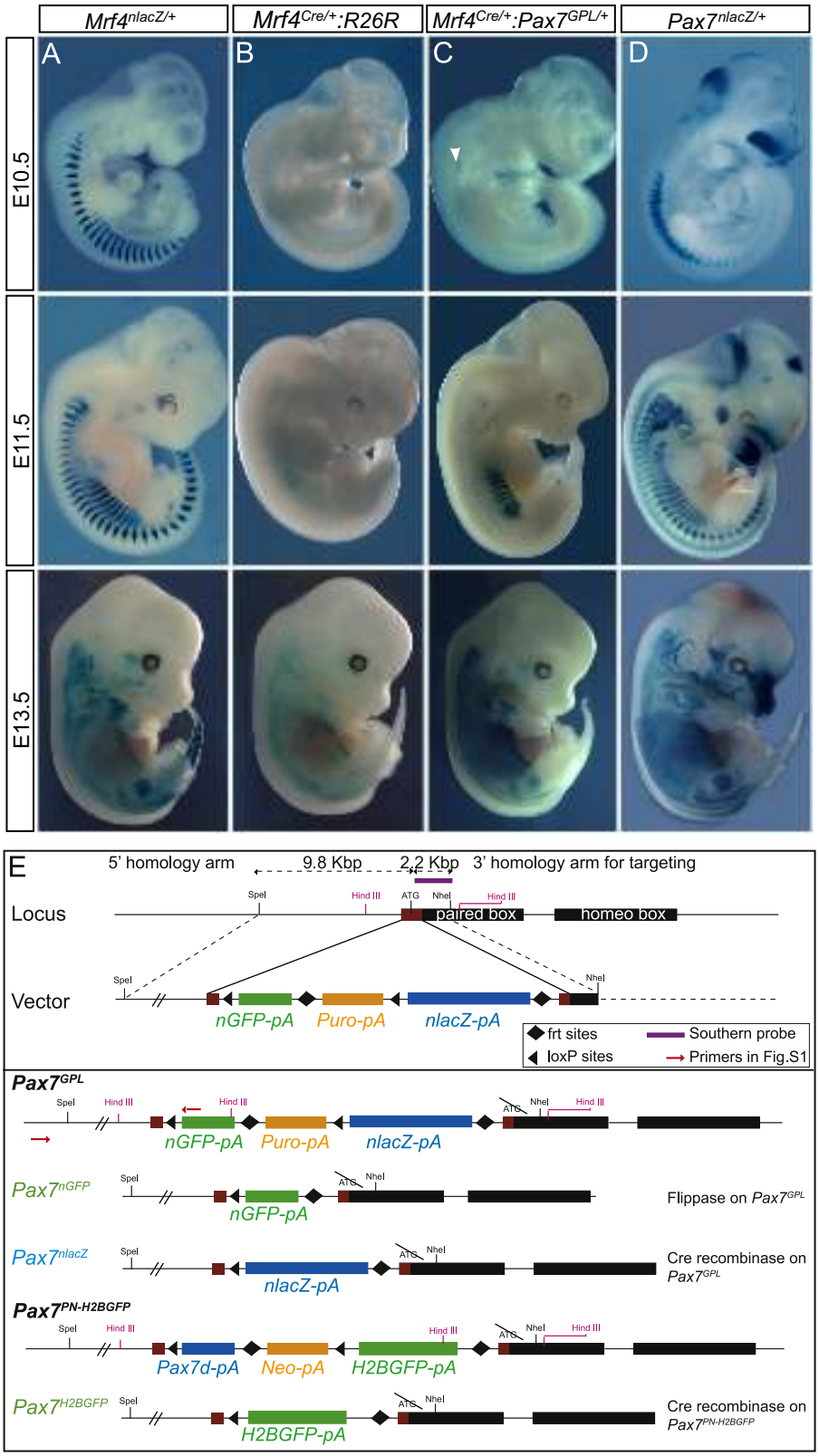

Fig. 2. Generation of Pax7 reporter lines with increased sensitivity for muscle lineage tracing studies. (A–D) Embryos of different embryonic days (E) stained with X-gal. (A) Pattern of *Mrf4* contemporary expression (*Mrf4*^{nlacZ}). (B) Readout of *Mrf4*^{Cre} expression from the ubiquitous *R26R*^{lacZ} reporter. (C) Tracing of *Mrf4* induction in Pax7^{+} progenitors with the *Pax7*^{GPL} reporter. Reporter signal is stronger and shows a higher degree of overlap with *Mrf4*^{nlacZ} than the *R26R*^{lacZ} reporter. Arrowheads highlight rare blue cells at E10.5. (D) Pattern of Pax7 expression from the *Pax7*^{nlacZ} allele. Note that the conditional activation of both the *R26R*^{lacZ} reporter and *Pax7* reporter by *Mrf4*^{Cre} (E11.5 panels B, C) is delayed with respect to *Mrf4*^{nlacZ} and *Pax7*^{nlacZ} expression (E10.5, E11.5 panels A, D). (E) Schematic of the generation of Pax7 reporter alleles by homologous recombination. On the Pax7 locus, the regions encoding the paired domain and homeodomain are represented. Maroon rectangle is the first exon, with ATG start codon flagged. The design of the targeting vector, allowed insertion of transgene in the first exon while deleting 36 bp of the exon downstream of the 5' UTR (57 bp), in order to remove two potential start codons. The placement of loxP sites and frt sites on the transgene in *Pax7*^{GPL} allows the use of this allele as a Cre-inducible stop-lacZ reporter. Moreover, as shown, the *Pax7*^{GPL} line was used to generate *Pax7*^{nGFP} and *Pax7*^{nlacZ} alleles by mating to either a ubiquitous Flippase (β-actin flippase) or Cre recombinase (PGK-Cre) lines, respectively. Identical targeting strategy was employed for the *Pax7*$^{PN\text{-}H2BGFP}$ allele. We aimed to generate a dual-purpose allele that would serve both as a conditional knock-out (cKO), by removal of a Pax7cDNA sequence (blue rectangle, Pax7d-pA), as well as a Cre-inducible H2BGFP reporter. Owing to lack of expression of the Pax7d transgene cassette, it could not be used as a cKO allele.

locus and in a Cre recombinase inducible manner, either nuclear β-galactosidase (*Pax7*^{GPL}→*Pax7*^{nlacZ}) or a fusion of Histone H2B and green fluorescent protein that localises to chromosomes (*Pax7*$^{PN\text{-}H2BGFP}$→*Pax7*^{H2BGFP}) (Fig. 2E). Flippase mediated recombination of the *Pax7*^{GPL} reporter (β-actin flippase; ActB:FLPe; (Rodriguez et al., 2000)) generates a *Pax7*^{nGFP} allele (Fig. 2E). The expression pattern of germline flipped or floxed reporters faithfully recapitulates that of the endogenous *Pax7* mRNA and protein during embryonic development (Figs. 3A, B; S2C), with the exception of the dorsal neural tube (Fig. S2D). As these reporters are under the control of endogenous *Pax7* promoter, they offer spatio-temporal specificity unlike the ubiquitous constitutive *R26R*^{lacZ} reporter (Soriano, 1999). In addition, the knock-in reporters also serve as *Pax7* null alleles (Fig. S3, shown only for *Pax7*^{nGFP}).

To further validate the *Pax7* lineage specific reporter lines, we compared the X-gal profile of *Mrf4*^{Cre}: *Pax7*^{GPL} embryos to that of embryos carrying the *R26R*^{lacZ} reporter as well as to *Pax7*^{nlacZ} and *Mrf4*^{nlacZ} embryos. Whereas *Pax7*^{nlacZ} and *Mrf4*^{nlacZ} expression showed a minimal overlap in the somites at E10.5, no significant expression was observed at this stage for any of the reporters, implying a delay in the activation of the reporters by *Mrf4*^{Cre} (Fig. 2A, D). However, by E13.5 a significant proportion of the Pax7^{+} stem/progenitor cells in the trunk and limbs were primed by *Mrf4* activity, with the labelling being considerably stronger with the *Pax7*^{GPL} compared to the *R26R*^{lacZ} reporter (Fig. 2B, C). In addition, the readout of *Mrf4*^{Cre} activity with the *R26R*^{lacZ} reporter constituted a subset of the expression detected with *Pax7*^{GPL}, which is unexpected for a reporter considered to be ubiquitous (Soriano, 1999).

We then investigated the expression of the *Pax7* lineage specific reporters in the skeletal muscle of adult animals. Here, a robust expression of *Pax7*^{nlacZ}, *Pax7*^{nGFP} as well as *Pax7*^{H2BGFP} was detected in satellite cells (Figs. 3D; S2E). Whereas, *Pax7*^{nGFP} was strictly restricted to satellite cells, *Pax7*^{nlacZ} and *Pax7*^{H2BGFP} were also expressed in a number of differentiated myonuclei (Figs. 3C; 4A; S2E) and *Pax7*^{H2BGFP} expression could be traced into differentiating nuclei in embryos as well (Fig. S2F). This discrepancy could reflect the relative stability of the reporters, where perdurance is noted in some cases. Importantly, reporter gene expression in both *Pax7*^{GPL} and *Pax7*$^{PN\text{-}H2BGFP}$ was strictly conditional on *Cre*-recombinase expression as reporter activity was absent in *Pax7*^{GPL} and *Pax7*$^{PN\text{-}H2BGFP}$ muscles (Fig. 3C, D). Expression of reporter genes was observed only when these lines were crossed to maternally controlled ubiquitous *Cre*-diver (*Tg:PGK-Cre*; (Lallemand et al., 1998)) to generate *Pax7*^{nlacZ} and *Pax7*^{H2BGFP} mice, respectively.

Thus, the *Pax7* lineage specific reporters are reliable and highly sensitive tools for muscle stem/progenitor lineage tracing studies compared to the commonly used ubiquitous reporter lines. Notably, these reporters allow us to define the developmental stage when *Mrf4* is active in Pax7^{+} myogenic cells.

Founders of satellite cells have activated the Mrf4 locus

To determine whether the *Mrf4* locus ever activated in founders of the satellite cell population, we examined *Mrf4*^{Cre}:*Pax7*$^{PN\text{-}H2BGFP}$ for reporter expression in adult skeletal muscle. Surprisingly, 99.8% of satellite cells were found to be H2BGFP^{+} in the TA muscle of the hindlimb as well as in a deep back muscles ($n=4$ animals, total of 860 nuclei; Fig. 4A, C). We then wondered whether this was the case for muscles at different anatomical locations, and with different embryonic origins. Whereas trunk and limb muscle

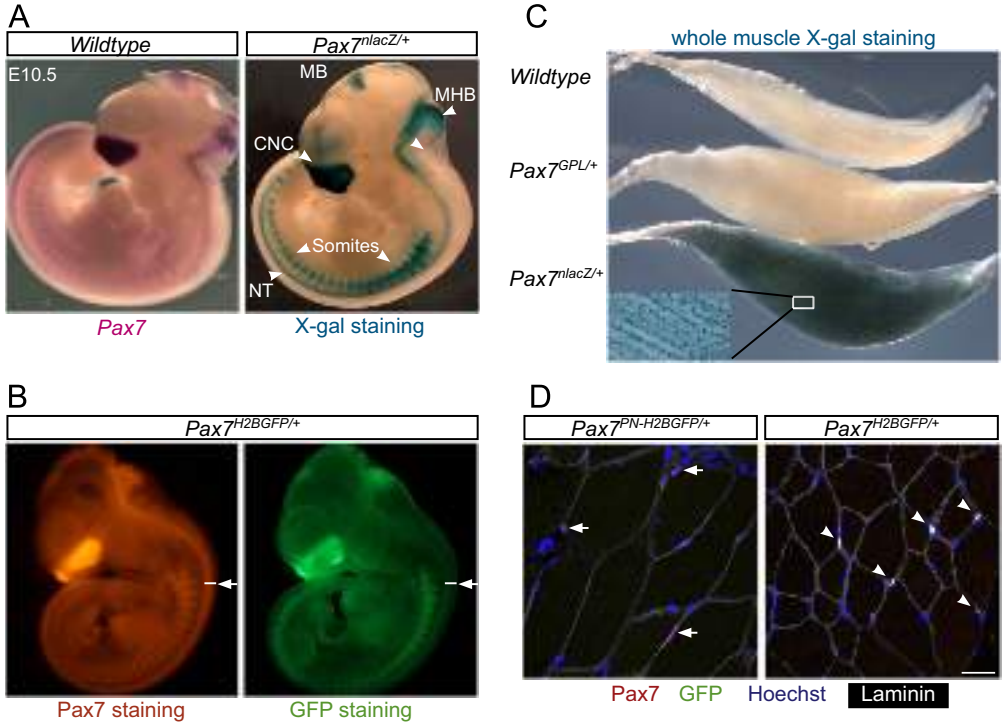

Fig. 3. Validation of *Pax7* reporters. (A, B) Expression pattern of *Pax7*^{nlacZ} and *Pax7*^{H2BGFP} faithfully recapitulate endogenous *Pax7* mRNA as well as protein expression. (A) Whole mount RNA *in situ* hybridisation of a *wild type* E10.5 embryo is compared to *Pax7*^{nlacZ} expression from an age-matched embryo. CNC, cranial neural crest; MB, a region of midbrain; MHB, midbrain–hindbrain boundary; NT, neural tube. (B) Pax7 and GFP whole mount double immunostaining on E10.5 *Pax7*^{H2BGFP} embryo. Dorsal extent of the Pax7 expression in neural tube is not reported by *H2BGFP*. (C, D) Expression of Pax7 conditional reporters is strictly Cre recombinase dependent. (C) *Extensor digitorum longus* muscles from indicated genotypes stained with a chromogenic substrate for β-galactosidase. Note, *Pax7*^{GPL} shows no leaky reporter expression ($n>3$ animals). *Pax7*^{nlacZ} expression is retained in differentiated myonuclei (inset). (D) Cross-section of *tibialis anterior* (TA) muscles, immunostained for Pax7 and GFP. *H2BGFP* expression is never observed in *Pax7*$^{PN\text{-}H2BGFP}$ muscles whereas in TA of *Pax7*^{H2BGFP}, generated using ubiquitous Cre-driver (PGK-Cre), all Pax7^{+} satellite cells express *H2BGFP*. Scale bar=25 μ.

satellite cells derive from somites (Armand et al., 1983; Gros et al., 2005), the satellite cells of head muscles are derived from cranial mesoderm ((Harel et al., 2009; Sambasivan et al., 2009); Fig. 4B). Even among head muscles, extraocular muscles (EOM) and pharyngeal arch-derived jaw and facial muscles have distinct genetic developmental programmes (Sambasivan et al., 2009). Analysis of the history of *Mrf4* activity in satellite cells of masseter (jaw muscle) and EOM tissue sections showed that >99% were H2BGFP^{+} (Fig. 4A, C; $n=4$ animals, 789 nuclei). Tongue muscles, which originate in somites but develop in the head environment (Christ and Ordahl, 1995; Tajbakhsh and Buckingham, 2000), had 93.3% of H2BGFP^{+} satellite cells (Fig. 4A, C; $n=253$ nuclei). Comparable results were obtained by immunofluorescence on cells following enzymatic digestion of the respective muscles (Fig. 4D, E; $n=2$ animals; TA, EOM and masseter; total $n=1282$ cells; data not shown).

Moreover, as different genetic loci are known to differ in their susceptibility to Cre-mediated recombination (Novak et al., 2000; Vooijs et al. 2001; Ma et al. 2008) we wanted to confirm the experiments performed in adult using a different reporter line

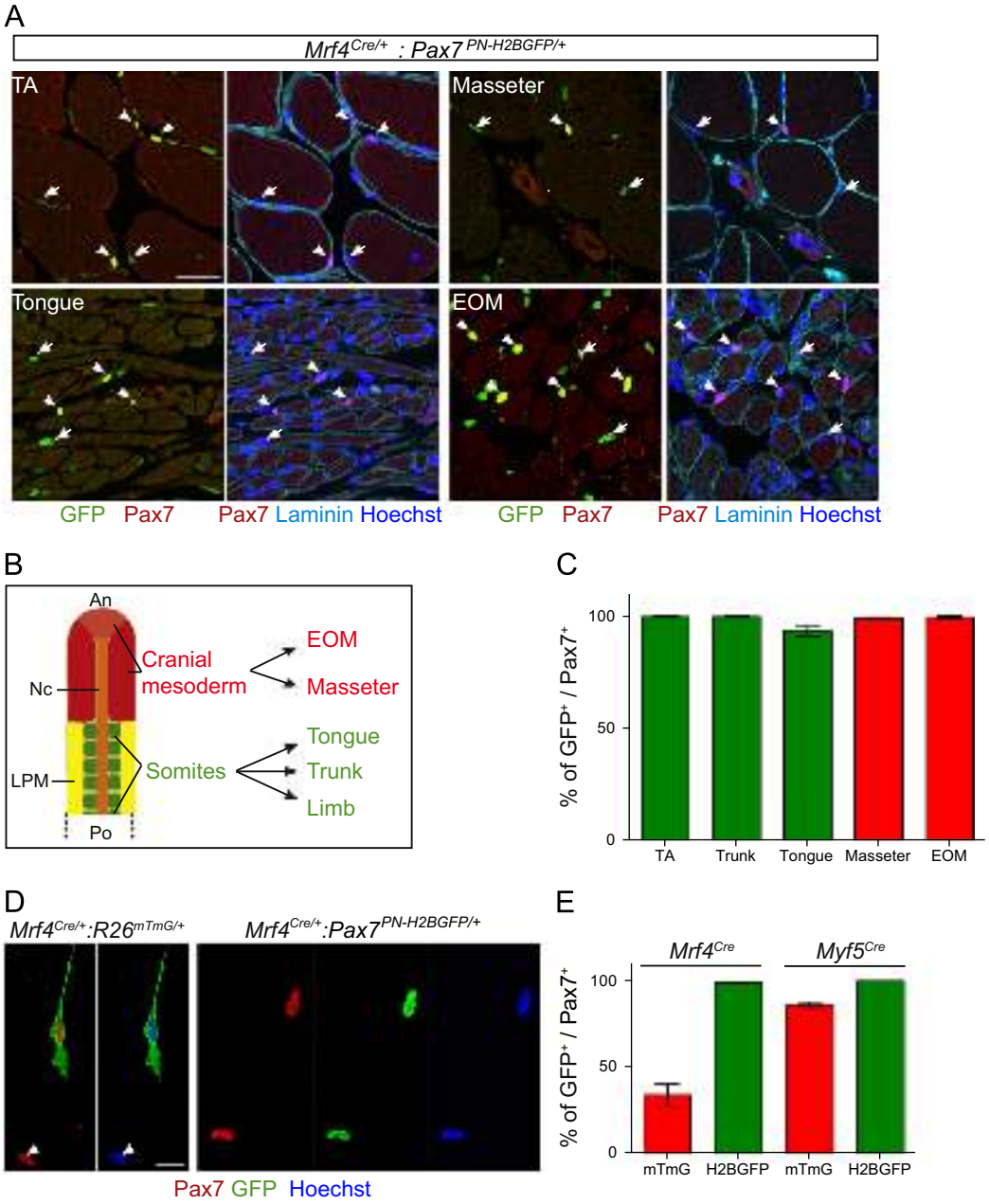

Fig. 4. History of *Mrf4* activation in satellite cells. (A) Genetic tracing into adult mice using the *Pax7*$^{PN\text{-}H2BGFP}$ allele reveals unexpected history of *Mrf4* expression in satellite cells. Cross-section of muscles of distinct embryological origins stained with GFP, Pax7 and laminin antibodies. Arrowheads show coexpression of Pax7 and GFP, arrows highlight persistence of GFP on differentiated myonuclei (Pax7^{-}). Scale bar, 25 μ. (B) Schematic showing the two distinct embryonic mesodermal sources of the various skeletal muscles and hence, satellite cells associated with them. An, anterior; Nc, notochord; LPM, lateral plate mesoderm; Po, posterior mesoderm; EOM, extraocular muscles. (C) Quantitation of the data shown in panel A. (D) Immunostaining for Pax7 and GFP on cells prepared by enzymatic digestion of Tibialis anterior (TA) muscles of *Mrf4*^{Cre}: *R26*^{mTmG} and *Mrf4*^{Cre}:*Pax7*$^{PN\text{-}H2BGFP}$ and plated overnight. Note the presence of membrane GFP negative cells (arrowheads) on the left panel. Scale bar=10 μ. (E) Percentage of recombined cells (GFP^{+}) over the total number of Pax7^{+} cells for *Mrf4*^{Cre} (quantitation of data on panel D) and *Myf5*^{Cre} (images not shown) with the *R26*^{mTmG} and *Pax7*$^{PN\text{-}H2BGFP}$ reporters. Note the higher recombination efficiency in TA with the lineage specific reporter (H2BGFP histograms, $n=2$ animals, 99.15% ± 0.10 for *Mrf4*^{Cre}; $n=2$ animals, 99.80% ± 0.08 for *Myf5*^{Cre}) in comparison to the ubiquitous reporter (mTmG histograms, $n=5$ animals, 33.58% ± 6.19 for *Mrf4*^{Cre}; $n=4$ animals, 86.12% ± 1.39 for *Myf5*^{Cre}).

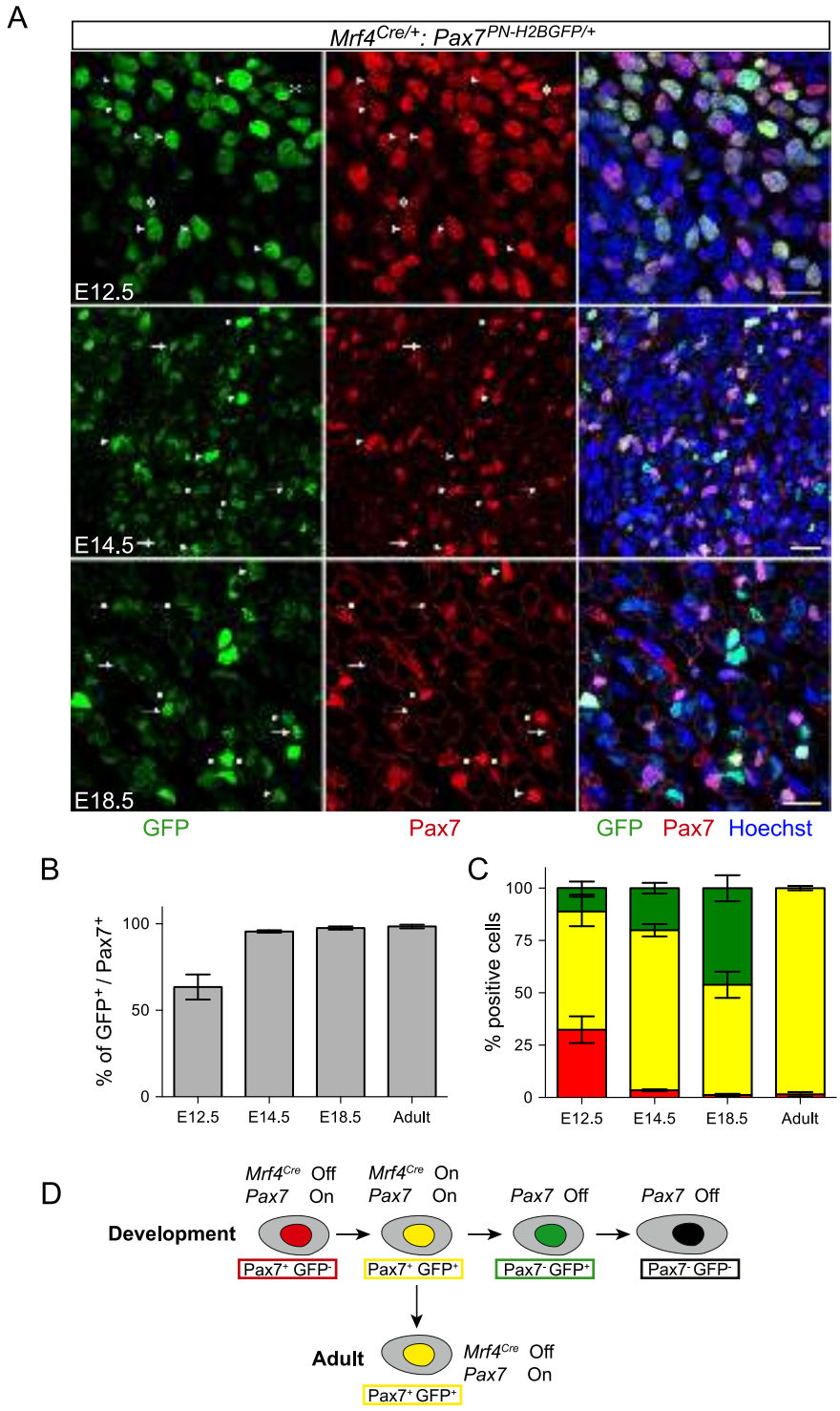

Fig. 5. *Mrf4* is induced in embryonic myogenic progenitors. (A) Immunostained sections at the trunk level of embryonic (E12.5), foetal (E14.5) and perinatal (E18.5) $Mrf4^{Cre}$:$Pax7^{PN\text{-}H2BGFP}$ muscle anlage in the myotome. All 3 panels of each row represent the same field. Arrows point to GFP only nuclei, asterisks flag Pax7 only nuclei and arrowheads mark double positive nuclei. Scale bar= 25 μ. (B) Histogram quantitating the proportion of $Pax7^+$ cells that are GFP^+. See text for the values. Note that nearly all Pax7+ cells were GFP+ by E14.5. Histogram for adult $Mrf4^{Cre}$:$Pax7^{PN\text{-}H2BGFP}$ (quantitation on cells prepared by enzymatic digestion of EOM muscles) was placed side-by-side for comparison. (C, D) Perdurance of H2BGFP reporter expression during development. (C) Quantitation of the single and double (Pax7, GFP) positive cells from $n=3$ embryos/ foetuses and $n=2$ animals for adult EOM. For E12.5, $n=514$ nuclei, for E14.5, $n=387$ nuclei for E18.5, $n=622$ nuclei and for adult EOM $n=440$ nuclei. Red histograms represent Pax7 only cells at E12.5 ($32.4\% \pm 6.4$), at E14.5 ($3.5\% \pm 0.5$), at E18.5 ($1.2\% \pm 0.5$) and adult ($1.53\% \pm 1.05$). Green histograms represent GFP only cells at E12.5 ($11.2\% \pm 3.2$), E14.5 ($20.1\% \pm 2.6$), E18.5 ($46.1\% \pm 6.2$). Yellow histograms represent $Pax7^+$ GFP^+ cells at E12.5 ($56.5\% \pm 7.0$), at E14.5 ($76.4\% \pm 2.9$), at E18.5 (52.6 ± 6.2) and adult ($98.5\% \pm 1.0$). Note that the difference in the % of $Pax7^+$ GFP^+ cells between panel B and C is because, panel B quantitates GFP^+ cells in $Pax7^+$ pool, while panel C quantitates the proportions in the combined pool of both $Pax7^+$ as well as GFP^+ cells (total number of nuclei). (D) Schematic illustrating the appearance of distinct pools of cells with respect to the expression of $Mrf4^{Cre}$ and Pax7. During development, $Pax7^{H2BGFP}$ reporter expression appears upon $Mrf4^{Cre}$ activation (yellow nucleus), persists temporarily in committed myogenic cells (green nucleus) then, extinguishes in differentiating cells (black nucleus). Postnatally, $Mrf4^{Cre}$ is not active in satellite cells, however, reporter expression follows that of *Pax7*. On/off indicate transcription or not from the $Mrf4^{Cre}$ and *Pax7* locus. The coloured squares indicate the readout by immunofluorescence of Pax7 and GFP proteins.

wherein *R26*^{mTmG} (*membrane Tomato-stop-membrane GFP*; (Muzumdar et al., 2007)) was crossed to *Mrf4*^{Cre} mice. In contrast to the *Pax7*$^{PN\text{-}H2BGFP}$ reporter, only 33.6 ± 13.8% of the satellite cells enzymatically isolated from adult TA were *R26*^{mTmG} reporter positive (Fig. 4D, E; $n=5$ animals, 5 TA, $n=1015$ cells). Notably, the frequency of recombined cells remained unchanged at least up to 8 months of age ($n=1$ animal, TA, EOM, masseter, total $n=453$ cells; data not shown). Thus, once again we noted a discrepancy in the frequency of GFP$^+$ satellite cells obtained with *Mrf4*^{Cre}*: R26*^{mTmG} compared to that of *Mrf4*^{Cre}*:Pax7*$^{PN\text{-}H2BGFP}$ (see Discussion). Nevertheless, this observation mirrored the difference in sensitivity of muscle embryonic progenitors labelled by *R26R*^{lacZ} compared to *Pax7*^{GPL} on whole mount embryos (Fig. 2B, C). To decipher whether the efficiency of recombination between the *Pax7* and *Rosa* reporters was a unique feature of the *Mrf4*^{Cre} allele or a rather generalised phenomena, we compared the recombination efficiency of *Pax7*$^{PN\text{-}H2BGFP}$ and *R26*^{mTmG} reporter alleles by *Myf5*^{Cre} (Haldar et al., 2008). Whereas 99.7 ± 0.19% of the satellite cells recombined the *Pax7*$^{PN\text{-}H2BGFP}$ reporter (Figs. 4E; S4; $n=2$ animals; TA, EOM, masseter; total $n=3108$ cells), 84.03 ± 1.08% cells of the satellite cells recombined the *R26*^{mTmG} reporter allele on cells enzymatically isolated from 6 to 8 week old mice (Figs. 4E; S4; $n=3$ animals, TA, EOM, masseter; total $n=2769$ cells). Notably, recombination efficiency of the *R26*^{mTmG} allele increased to almost 100% at 15 months (Fig. S4B; $n=2$ animals; EOM, masseter; total $n=1261$ cells). In summary, the recombination efficiency by *Myf5*^{Cre} was nearly 100% with the lineage specific reporter. Although the difference in recombination between *R26*^{mTmG} and *Pax7*$^{PN\text{-}H2BGFP}$ reporters was small with *Myf5*^{Cre}, it was dramatic (about 3 fold) with *Mrf4*^{Cre}. Moreover, the rate of recombined *Myf5*^{Cre}*: R26*^{mTmG} cells increased over time in striking contrast to the *Mrf4*^{Cre}*: R26*^{mTmG} mice, which remained low (data not shown; see discussion for physiological relevance).

Together, these observations show that an overwhelming majority of satellite cell founders, irrespective of their embryonic origin, activated the *Mrf4* locus. Cre protein driven by *Mrf4*^{Cre} was not present in juvenile and adult stem/progenitor cells (Fig. 1; (Keller et al., 2004a)), therefore we hypothesised that *Pax7*$^{PN\text{-}H2BGFP}$ reporter expression in adult skeletal muscle satellite cells from *Mrf4*^{Cre} mice reflects historical Cre expression in the founder population likely during embryogenesis.

Mrf4 genetic tracing reveals a lineage continuum between embryonic and adult muscle stem/progenitors

To examine *Mrf4*^{Cre} activity in more detail, we co-immunostained cryosections of *Mrf4*^{Cre}*:Pax7*$^{PN\text{-}H2BGFP}$ samples at E12.5 (embryonic), E14.5 (foetal) and E18.5 (perinatal) stages with anti-GFP and anti-Pax7 antibodies. To quantify the extent of co-expression and the possible appearance of new H2BGFP negative cells (i.e. not *Mrf4* primed) at later stages, which would argue against a lineage continuum model, we focused on myotome or myotome-derived anlage of trunk muscles. At E12.5, a major proportion of Pax7$^+$ cells in the myotome were GFP$^+$ (63.5% ± 7.24;

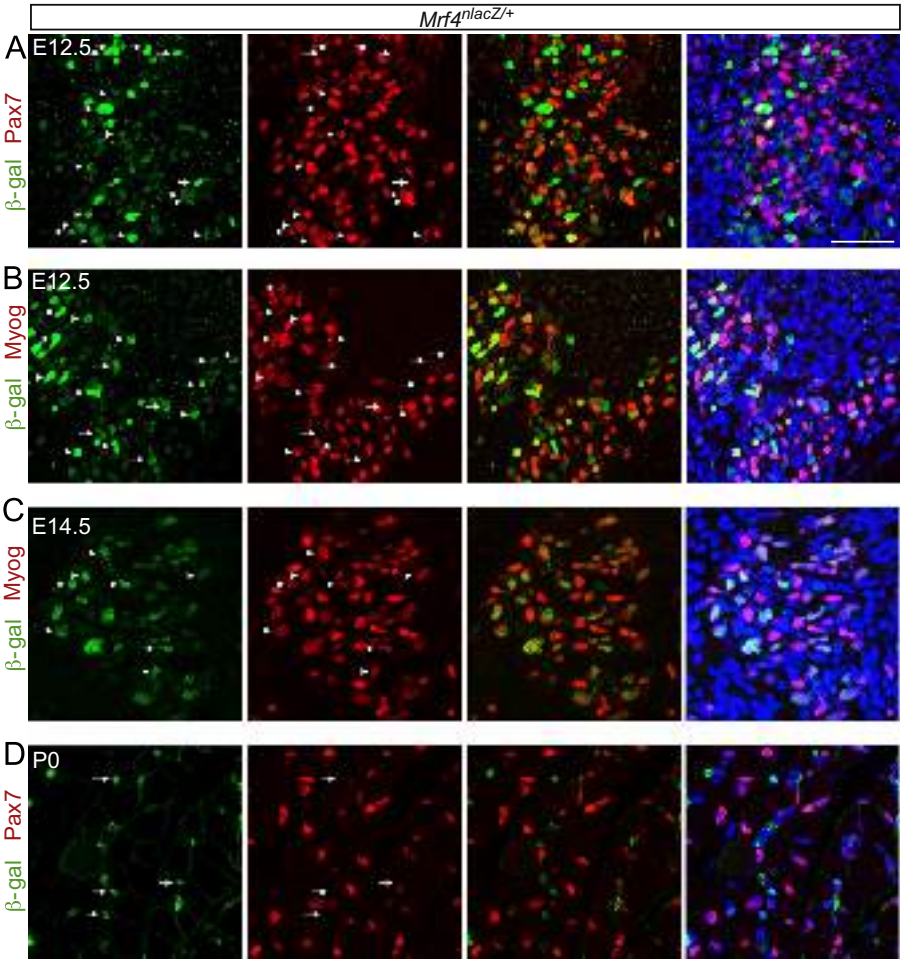

Fig. 6. *Mrf4* induction in progenitors is restricted to the embryonic myogenic phase. (A–D) Immunostaining with anti-β-gal and anti-Pax7 (A, D) or Myog (B, E) antibodies on *Mrf4*^{nlacZ} sections from embryonic (E12.5), foetal (E14.5) and post-natal (P0) phases. Sections for the top panels (A–C) were obtained from trunk at forelimb level, the P0 panels show a hindlimb section. Arrowheads point to double positive nuclei; arrows mark β-gal only expressing nuclei. Scale bar = 25 μ.

$n=3$ embryos; 461 nuclei) and nearly all Pax7$^+$ cells were GFP$^+$ by the early foetal stage E14.5 (95.6% ± 0.7; $n=3$ embryos; 304 nuclei) (Fig. 5A, B). The proportion of double positive cells in the trunk remained high at E18.5 (Fig. 5A, B; 97.6% ± 0.9; $n=3$ embryos; 317 nuclei). Importantly, Pax7$^+$ cells not expressing GFP were rarely or never observed after E14.5 until birth (Fig. 5B–D). We observed, however, a steady increase in the number of GFP$^+$/Pax7$^-$ cells over the course of development (Fig. 5C), indicating that the H2BGFP reporter is more stable than Pax7 protein. Accordingly, some GFP$^+$ cells in the myotome were Myog$^+$ showing that they were differentiated (Fig. S2F). Given that Pax7 and Myog rarely co-express, this observation suggests a temporary perdurance of *H2BGFP* from *Pax7^{H2BGFP}*. In adult muscle, we did not observe GFP$^+$/Pax7$^-$ cells (Fig. 5B, C; 0.05% ± 0.05%; $n=2$ animals, TA, EOM, masseter; $n=1282$ nuclei), indicating that the perdurance of GFP expression is a transient event during development. Therefore, GFP expression from the recombined *Pax7^{H2BGFP}* locus faithfully follows endogenous *Pax7* promoter activity.

Taken together, these observations strongly suggest that the majority of Pax7$^+$ cells have been primed by *Mrf4* expression at the end of embryonic phase of myogenesis, and no new wave of Pax7$^+$ Mrf4$^-$ stem/progenitors appears to arise in the subsequent foetal and perinatal myogenic phases.

Mrf4 expression is confined to embryonic muscle progenitors

We next asked whether *Mrf4* activation occurs only in the Pax7$^+$ stem/embryonic progenitors (contemporary expression) or in progenitors of foetal and perinatal developmental phases as well (cumulative expression). We made use of the *Mrf4^{nlacZ}* allele, which marks contemporary expression from the *Mrf4* locus as opposed to the *Mrf4^{Cre}:Pax7$^{PN\text{-}H2BGFP}$* reporter assay used above, which provides a cumulative record of *Mrf4* expression.

At E12.5, we observed some β-gal$^+$ cells co-expressing Pax7 or Myog in the myotome (Fig. 6A, B). Notably, among the different muscle anlage derived from the myotome, the proportion of β-gal co-expression with Pax7 or Myog appeared to vary significantly thereby precluding quantifications (Fig. S5A, B). Moreover, in some anlagen β-gal was undetectable (Fig. S5A, B). Therefore, *Mrf4* activation in Pax7$^+$ stem/progenitors occurs asynchronously in embryonic muscle progenitors of different developing muscle masses. Overall, the proportion of β-gal$^+$ nuclei among Pax7$^+$ stem/progenitors (contemporary *Mrf4* expression) appeared to be minor (Fig. S5A, B) and far below the average 63.5% overlap quantitated from *Mrf4^{Cre}:Pax7$^{PN\text{-}H2BGFP}$* (cumulative record of *Mrf4* expression) at the same stage (Fig. 5B). By E14.5, rare or no co-expression of β-gal could be observed in Pax7$^+$ cells even when using the sensitive *Tg:Pax7nGFP* mouse line to monitor Pax7 expression (Fig. S6A, B). In contrast, the majority of β-gal$^+$ cells co-expressed Myog (Fig. 6C). Similarly, mutually exclusive Pax7 and β-gal staining was observed in newborns (Fig. 6D; $n=3$ pups, a total of 453 nuclei). Both E14.5 and P0 data are consistent with our previous report showing that *Mrf4^{nlacZ}* does not mark Pax7$^+$ cells in the foetus from E15.5 (Kassar-Duchossoy et al., 2005) and that later, Mrf4 functions as a differentiation factor.

To address the expression of *Mrf4* in Pax7$^+$ cells and myotubes by an independent method, we directly measured the expression of *Mrf4* in the Pax7$^+$ stem/progenitors isolated by FACS from embryos of *Tg:Pax7nGFP* mice. Quantitative RT-PCR analysis revealed extremely low levels of *Mrf4* mRNA expression in the Pax7nGFP$^+$ cells isolated from trunks of E12.5 as well as E17.5 embryos when compared to adult muscle fibres (Fig. S5C). This indicates that *Mrf4* is induced transiently and asynchronously in the embryonic Pax7$^+$ stem/progenitors such that at the population level the mRNA is undetectable.

In the experiments above, we observed that: (i) nearly all Pax7$^+$ progenitors had activated *Mrf4* by the end of the embryonic phase (E14.5); (ii) this proportion remained stable in the late foetal phase (E18.5). Given that contemporary expression of *Mrf4* in stem/progenitors was virtually undetectable in the foetal phase, these observations suggest that embryonic activation of *Mrf4* results in priming of the majority of the Pax7$^+$ stem/progenitor population and that no new Pax7$^+$ stem cells arise from Mrf4$^-$ founders. This,

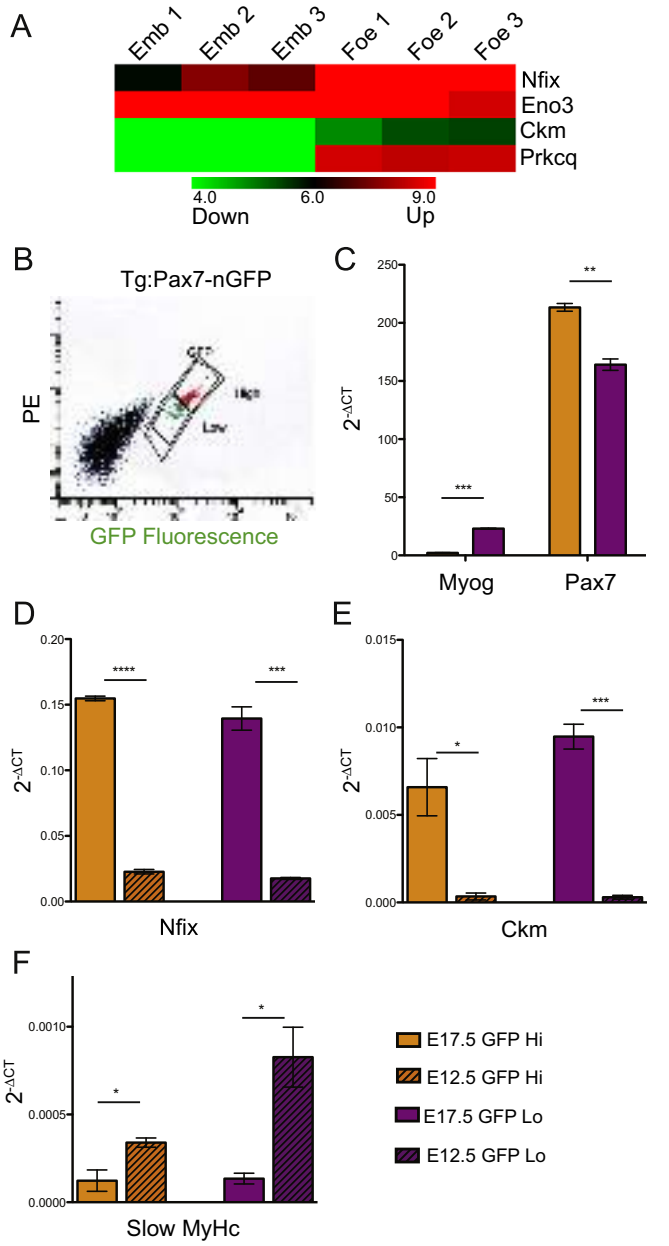

Fig. 7. Upstream stem/progenitors of both embryonic as well as foetal myogenic waves express phase-specific markers. (A) Heatmap revealing up regulation of foetal phase-specific genes in Pax7nGFP$^+$ cells isolated from E17.5 limbs (Foe 1-3) when compared to those from E12.5 limb buds (Emb 1-3). Data extracted from microarray transcriptome comparison (R.S., S.T. unpublished). (B) FACS profile to indicate the Pax7nGFP^{High} (upstream stem/progenitor; GFP Hi) and Pax7nGFP^{Low} (committed myoblast; GFP Lo) cells sorted for RT-qPCR analyses. *Y*-axis, in logarithmic scale as *X*-axis, represents spectral cross-over of green fluorescence in the red channel (PE). (C) Expression levels ($2^{-\Delta CT}$) of *Myog* and *Pax7* relative to levels of reference (*TBP*; TATA binding-protein) transcripts. Comparison between Pax7nGFP^{Hi} and Pax7nGFP^{Lo} cells from E17.5 limbs. (D–F) Expression levels of *Nfix* and *Ckm* (foetal-specific markers) as well as slow *MyHc* (embryonic phase-specific gene) in indicated cell populations. Samples compared are GFP Hi of foetus (E17.5) vs. embryo (E12.5) and GFP Lo of E17.5 vs. E12.5.

in turn, argues against the possibility that the temporally distinct muscle stem/progenitors derive from phase specific naïve founder cells.

Upstream embryonic and foetal stem/progenitors express stage specific markers

To further examine the issue of lineage relationships among the developmental muscle stem/progenitors, we sought to investigate the molecular signature of the upstream Pax7^{+} population from both the embryos and foetus (E17.5) with respect to the foetal specific transcription factor Nfix, and Nfix-regulated genes. A previous profiling study that identified differential embryonic and foetal marker expression had been performed with a heterogeneous *Myf5*$^{GFP/+}$ population (Biressi et al., 2007b), comprising both upstream progenitors as well as committed and differentiating myoblasts (Gayraud-Morel et al., 2012). We compared the transcriptomes of GFP^{+} cells isolated from *Tg:Pax7nGFP* E12.5 embryos and E17.5 foetuses and found a similar trend of expression of Nfix and other phase-specific genes as it had been reported with the *Myf5*$^{GFP+}$ populations ((Biressi et al., 2007b); Fig. 7A). Next we fractionated the population into *Pax7nGFP*^{Hi} (top 50%) and *Pax7nGFP*^{Lo} (bottom 50%) by fluorescence activated cell sorting (FACS; Fig. 7B). In agreement with our previous studies, both in the adult and during development, we show here that Pax7^{Hi} represents a pool upstream in the lineage cascade, i.e., high *Pax7* and undetectable levels of downstream genes such as *Myog* (Mourikis et al., 2012b; Rocheteau et al., 2012); Fig. 7C). Surprisingly, not only the Pax7^{Lo} committed myoblasts, but also the upstream Pax7^{Hi} cells expressed the phase-specific commitment markers at both embryonic and foetal stages. We observed higher levels of slow MyHC expression in embryonic Pax7^{Hi} cells as well as in committed Pax7^{Lo} myoblasts, when compared to those populations from the foetus. Similarly, *Nfix* and *Ckm* were upregulated both in foetal Pax7^{Hi} and Pax7^{Lo} cells relative to the respective embryonic populations. This implies that the upstream population is committed to generating developmental phase-specific muscle cells, though the cellular resolution of our analysis is limited. Nevertheless, taken together with (a) the near complete activation of *Mrf4* in embryonic stem/progenitors and the absence of *Mrf4*$^{+}$ stem/progenitors in all subsequent phases of myogenesis, as well as satellite cells and (b) our recent report that embryonic muscle progenitors arrested in differentiation by ectopic Notch signalling adopt foetal character later (Mourikis et al., 2012a), our data support a linear progression of the stem/progenitor lineage during the successive waves of myogenesis, i.e., foetal progenitors arise from embryonic muscle stem/progenitors and so on (see Discussion below).

Discussion

How adult tissue specific stem cells emerge during ontology is a major unresolved question in developmental biology. The finding that adult skeletal muscle stem cells exhibit heterogeneity in behaviour has lead to the suggestion that the extent of priming of prenatal muscle stem cells by the determination genes *Myf5*, *Myod* and *Mrf4* predisposes the adult counterparts of these muscle founder cells to assume different states of myogenic commitment. The discordant results obtained from previous Cre-lox strategies using *Myf5* (Kuang et al., 2007) and *Myod* (Kanisicak et al., 2009) genetically modified mice raised the question: does *Mrf4* priming occur in emerging stem cells prenatally and postnatally? Here we report that priming of muscle founder stem cells by *Mrf4* expression occurs extensively as this population emerges in the embryo, and this does not occur further from foetal stages. Our observations lead us to propose that signals that prompt unidirectional commitment by potent cell fate regulators act at the earliest stages of muscle stem cell emergence, yet these cells retain phenotypic flexibility with the capacity to return to a less committed cell state in the adult. This major conclusion from our work was revealed uniquely by generating muscle lineage specific reporter lines in the *Pax7* locus.

Use of Cre recombinase strategy in lineage analysis

Evaluation of the expression of the muscle determination genes or other lineage markers in the developmental history of satellite cells requires methods that allow permanent and irreversible readout overtime. While Cre is expressed in temporally and spatially defined patterns, recombination of a Cre-dependent reporter is an on/off readout in which only the progenitors having reached an appropriate threshold of Cre expression can be activated (Ma et al. 2008). In this study, *Mrf4* priming of nearly all founder stem cells was observed using a newly generated lineage specific *Pax7* reporter knock-in mouse. In contrast, less than half of the founder cells were marked by *Mrf4*^{Cre} when a widely used *Rosa* reporter readout was employed (see Fig. 4). As a comparison we evaluated the efficiency of *Myf5*^{Cre}, an already described driver, to recombine *Pax7*$^{PN\text{-}H2BGFP}$ and *R26*^{mTmG} loci. Similar to *Mrf4*^{Cre}, although to a much lesser extent, we found different recombination rates depending on the reporter line used (see Figs. 4; S4). A likely explanation for the discrepancy is that the lineage specific locus is transcriptionally more active, therefore more accessible and thus can be activated by lower levels of Cre or more transient exposure to Cre. Another possibility is the difference in the levels of lineage-specific versus ubiquitous reporter gene expression. The stark differences obtained with the different reporter lines, in particular with *Mrf4*^{Cre}, underscores the importance of exercising caution in interpreting lineage relationships with the widely used ubiquitous reporters. Indeed, differences between lineage specific and ubiquitous reporters are not restricted to the myogenic lineage (Ma et al., 2008).

Interestingly, both the present study and a previous study using the *R26*^{YFP} reporter with a distinct *Myf5*^{Cre} allele (Kuang et al., 2007), revealed a *Myf5*^{Cre}*-Rosa* reporter negative population of about 10% of the satellite cells, and these were reported to exhibit more stem-like properties. Along this line, our *Mrf4*^{Cre} and *Myf5*^{Cre} results that virtually all satellite cells have recombined the *Pax7*$^{PN\text{-}H2BGFP}$ reporter does not exclude the possibility of functional heterogeneity in the progenitor pool. In the case of *Mrf4*, whether functional heterogeneity might be revealed by the *Mrf4*^{Cre}*:R26*^{mTmG} negative population (about 70% of the satellite cells), which historically expressed lower levels of Cre, should be examined further. In addition, our observation that *Pax7*$^{PN\text{-}H2BGFP}$ reporter expression levels follow that of the endogenous *Pax7* locus, indicates that this reporter is a potentially useful readout of the heterogeneity in the adult pool. In fact, our preliminary results reveal the existence of Pax7^{Hi} and Pax7^{Lo} satellite cell populations among the 100% of *Pax7*$^{PN\text{-}H2BGFP}$ recombined cells (data for *Myf5*^{Cre}; S.T., G.C., I.L.R., unpublished observations).

It is important to note that the expression of a knocked-in Cre recombinase simply reflects the active status of the locus and not necessarily the expression of the endogenous protein from it (see (Tajbakhsh, 2009)). Therefore, the conclusions from using this strategy need to take this point into consideration. The *Mrf4*^{Cre} allele employed here, was generated and used in a previous report as a differentiated muscle cell-specific Cre driver (Keller et al., 2004a, 2004b). Our results clearly show that, while *Mrf4* expression is undetectable in adult stem/progenitor cells, it is expressed and functionally active in the embryonic myogenic cells. In another study the same *Mrf4*^{Cre} allele was used to eliminate

differentiated muscle cells and differentiated fibres were found to be lost during the foetal period (Haldar et al., 2008). That study assumed no loss of progenitors in the embryonic phase as the muscle continued to develop till E18.5. We reasoned that this could be due to the use of the *R26*$^{eGFP\text{-}DTA}$ allele (Wu et al., 2006), which like the *R26*^{mTmG} or *R26R*^{lacZ} alleles in our study (Muzumdar et al., 2007; Soriano, 1999), recombined less efficiently than the *Pax7* locus and hence might not have depleted all of the *Mrf4* expressing progenitors. We have confirmed this point experimentally by analysing *Mrf4*^{Cre}*: R26*$^{eGFP\text{-}DTA}$ foetuses (stronger *R26*$^{stop\text{-}DTA}$ allele (Ivanova et al., 2005)). Rather than eliminating the Pax7^{+} population, as would be excepted from the lineage study reported here, the trunk muscle of these foetuses contained significant numbers of Pax7^{+} cells thereby exposing weaknesses in using this combination of genetic tools (Fig. S7).

Antecedence of Mrf4 activity reflects the regulatory cell state of satellite cell founders

Satellite cells are defined by their location between host myofibre membrane and its basement membrane, as well as by marker expression such as *Pax7*. Such cells, that fit both the anatomical and molecular characteristics, arise during late foetal stages in mouse. While some of these cells differentiate to contribute to prenatal and postnatal muscle growth, the remaining enter mitotic quiescence by the young adult stage (see (Tajbakhsh, 2009)). Based on snapshots of expression of upstream markers *Pax3*/ *Pax7* and the determination genes, *Myf5*/*Myod*/*Mrf4* (Kassar-Duchossoy et al., 2005; Relaix et al., 2005), Pax^{+}MRF^{-} cells associated with muscle anlagen were observed throughout development and identified as the founders of satellite cells. This appeared to suggest that satellite cells arise from a naïve Pax^{+}MRF^{-} pool of ancestral cells.

The lineage priming results reported for *Myf5* and *Myod* using Cre-lox tracing could be reconciled with genetic cell ablation experiments. Interestingly, Myod^{+} embryonic muscle progenitors that never expressed *Myf5*^{Cre} were reported to sustain developmental myogenesis when *Myf5*$^{+}$ cells are ablated (Gensch et al., 2008; Haldar et al., 2008). It can be argued that the former population generates the minority *Myf5*-negative satellite cell pool identified previously (Kuang et al. 2007). However, based on the fact that virtually all adult satellite cells have recombined the *Pax7*$^{PN\text{-}H2BGFP}$ reporter in a *Myf5*^{Cre} dependent manner, it could well be that the *Myf5*-negative/*Myod*-only embryonic muscle progenitors described previously had been actually low *Myf5* expressing, thus insufficient to activate *Rosa*-driven reporters or DTA alleles. Whatever the case, our finding that almost all satellite cells have a history of *Mrf4* expression strongly indicates that the MRF activation status of the founders in the embryo does not in itself explain the functional heterogeneity in the satellite cell population (Fig. 8). Following on this point, the use of mouse strains carrying simultaneously a *Rosa*-based and lineage specific reporter (i.e. *Mrf4*^{Cre}*: Pax7*^{PNH2BGFP}*: R26*^{mTmG}) could be useful to clarify issues regarding heterogeneity.

Finally, a number of experiments from our laboratory are not consistent with the notion that apparently more committed satellite cells, as gleaned from their transcriptome, are less potent as self-renewing stem cells. These observations do not involve Cre-lox lineage tracing. Firstly, satellite cells isolated and fractionated into Pax7nGFP^{Hi} and Pax7nGFP^{Lo} appear less and more commited to the myogenic lineage, respectively (Mourikis et al., 2012b; Rocheteau et al., 2012). Yet, upon serial transplantation into injured muscle, both of these populations were comparable in their regeneration and self-renewal efficiency (Rocheteau et al., 2012). Secondly, endogenous *Myf5*$^{+/-}$ satellite cells, which appear more lineage primed and commited to the muscle lineage at the transcriptome level, unexpectedly show a higher potential for self-renewal upon transplantation (Gayraud-Morel et al., 2012). Taken together with the results presented here, we conclude that founders of satellite cells had explored the MRF^{+} regulatory cell state but are not anchored to the commitment state.

These findings still leave the observations with *Myf5*^{Cre} tracing (Kuang et al., 2007) to be reconciled. One possibility is that YFP^{+} cells from *Myf5*^{Cre}*: R26*^{YFP} in those experiments represent not only historic *Myf5* activity, but also contemporary *Myf5* expression in adult satellite cells. Evidence for this possibility comes from the fact that we have observed an increase in the percentage of recombination in *Myf5*^{Cre}*: R26*^{mTmG} animals from about 85% at 6–8 weeks to almost 100% at 15 months, supporting the view that persistent, active *Myf5* transcription is explored by all satellite cells. In addition, our recent report shows convincingly that a great majority of satellite cells (90%) express Myf5 protein (Gayraud-Morel et al., 2012). Absence of Myf5 protein might explain the better self-renewal manifested by YFP^{-} satellite cells in the transplantation assay by Kuang et al. (2007), in fact, we showed recently that heterozygous *Myf5* mutant satellite cells with lower levels of Myf5 self-renew better than wildtype satellite cells (Gayraud-Morel et al., 2012). In constrast to the observation for *Myf5*^{Cre}, we did not observe any increase in recombination

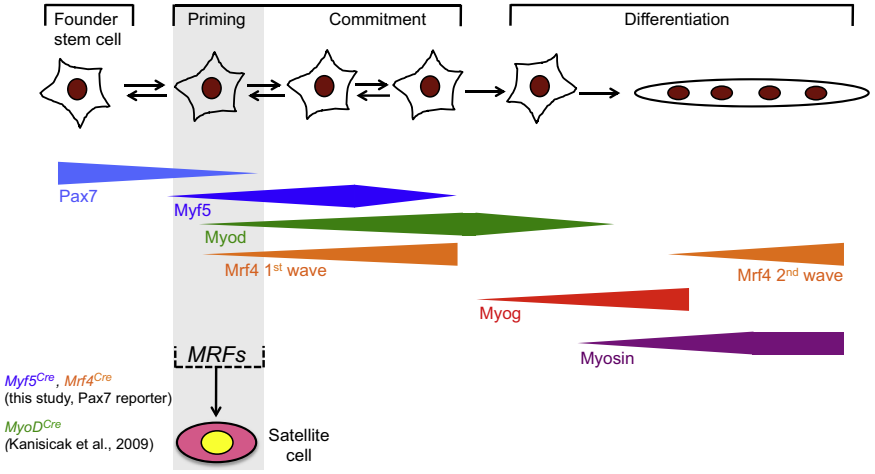

Fig. 8. (A) Regulatory cell state of founders of satellite cells. The top line illustrates lineage progression of progenitors during myogenesis. The shaded box indicates that almost all satellite cells are derived from MRF^{+} founders (priming). The corollary is that MRF induction in founders does not curtail the stem cell potential of adult muscle satellite cells. It must be noted that MRF^{+} status revealed by Cre-lox strategy does not reflect the expression of functional MRF proteins.

in *Mrf4^{Cre}: R26^{mTmG}* animals over time (S.T., I.L.R., G.C., data not shown), further supporting the conclusion that *Mrf4* transcription is absent in adult satellite cells.

Taken together, we propose that expression of MRFs in founders during development does not limit the 'stemness' of adult satellite cells. We also suggest that the functional heterogeneity in adult satellite cell compartment is likely causally linked to both the current expression status of MRFs (in particular Myf5) as well as to historical MRF expression.

Linear lineage relationship among developmental muscle progenitors

Muscle tissue in mice begins to form from about E10.5 and continuously develops and grows till full adult size is achieved. Up to 3 weeks after birth, the growth is brought out by the stem/progenitor cell population. Understanding the emergence and evolution of this population is central to understanding muscle development. Our data suggests that foetal stem/progenitors derive from the population that contributed to embryonic muscle growth and not from a new upstream population (Supplementary Fig. S8). We note that in our strategy using a *Pax7* reporter, Pax3^{+}/Pax7^{-} embryonic muscle stem/progenitors would not be traceable. Thus, a *Pax7* reporter might not reflect the proportion of total muscle progenitors expressing *Mrf4*. However, Pax3^{+} myogenic cells rapidly diminish and exhaust by the foetal period (Goulding et al., 1991; Horst et al., 2006). In addition, we obtain virtually identical lineage specific reporter readouts for trunk and head muscles, the latter having a different developmental origin, which is Pax3 independent. Therefore, we argue that our approach allows us to address the lineage relatedness of embryonic and foetal progenitors.

Our data also suggests that such a direct lineage relationship extends to satellite cells. However, a recent report (Dellavalle et al., 2011) shows that in the post-natal period (around 1st week after birth) of growth, satellite cells could arise from *Alpl* (alkaline phosphatase) expressing cells associated with blood vessels. Pw1 (a stress related protein) expressing interstitial population has also been proposed to enter the myogenic pool during post-natal growth (Mitchell et al., 2010). To reconcile these reports with our data that almost all adult satellite cells have activated *Mrf4*, one has to assume that a wave of *Mrf4* activation occurs during this postnatal period in these 'outsider cells' entering the muscle lineage. Alternatively, we must note that the contribution of vessel-associated cells to satellite cells is not uniform in all muscles (Dellavalle et al., 2011). Similarly, we find rare *Mrf4*$^{-}$ satellite cells in most of the muscles analysed and up to 6.7% *Mrf4*$^{-}$ satellite cells in tongue. It is possible that these Mrf4^{-} satellite cells represent those derived from the vessel-associated cells, which unlike the muscle progenitors from the embryo, did not activate *Mrf4*.

A caveat in our interpretation favouring a linear lineage is that we use absence of an *Mrf4*$^{-}$/Pax7^{+} population in foetal and later stages to argue that all of Pax7^{+} muscle progenitors in the embryo have already induced *Mrf4*. It could be argued that the foetal Pax7^{+} population emerges from an MRF^{-}/Pax7^{+} pool, but transiently induces *Mrf4* gene expression and hence, escapes detection as an *Mrf4*$^{-}$/Pax7^{+} population. However, another recent work strongly buttresses his argument. The study demonstrates that embryonic progenitors prevented from differentiating into embryonic muscle, due to forced expression of constitutively active intracellular domain of Notch, subsequently acquire foetal identity (Mourikis et al., 2012a), thus favouring the linear lineage model proposed here.

Conclusions

Firstly, our study underscores the importance of using combinations of reporter mice for readouts in genetic lineage studies. Secondly, we propose that embryonic Pax7^{+} muscle progenitors, and majority of the adult muscle satellite cells, could be linearly lineage related. Finally, we conclude from our results that the regulatory state of embryonic founder muscle stem cells, in terms of extent of commitment into the myogenic lineage during development, does not affect the stem cell potential of adult muscle satellite cells. Our findings could be extrapolated to stem cells in other tissue compartments and, in general, is significant to understand the emergence of adult stem cell populations.

Experimental procedures

Animals

Animals were handled as per European Community guidelines. Mouse lines with mutant alleles, *Myf5^{nlacZ}*, and *Myf5^{loxp}: Mrf4^{nlacZ}* (referred to as *Mrf4^{nlacZ}* throughout the article) were described previously (Kassar-Duchossoy et al., 2004). Generation of *Pax7^{GPL}* and Pax7$^{PN\text{-}H2BGFP}$ lines is described in the next section. For *Mrf4^{Cre}*, see (Keller et al., 2004b), *R26R^{lacZ}* (Soriano, 1999), *R26$^{eGFP\text{-}DTA}$* (Jackson; (Ivanova et al., 2005)), *R26^{mTmG}* (Jackson 007576; (Muzumdar et al., 2007)), *Myf5^{Cre}* (Haldar et al., 2008), *Tg: Pax7nGFP* (Sambasivan et al., 2009). Mouse mutants were genotyped and interbred as described (Kassar-Duchossoy et al., 2004). For all *Pax7* alleles, the genotyping was done with the following primers. Forward primer on SV40 polyA signal sequence at the 3' end of all the transgenes: 5' ccacacctccccctgaacctgaaacataaa 3' and reverse primer on the *Pax7* locus immediately downstream of the insertion: 5' gaattccccggggagtcgcat cctgcgg 3'.

Generation of Pax7 reporter lines

The targeting vectors were designed to replace 36 bp of the first exon downstream of the 5' UTR (57 bp) with the reporter constructs, thus generating knock-out alleles for *Pax7*. The Pax7-GPL targeting vector was designed with a nuclear GFP protein sequence, a puromycin selection cassette and a nuclear β-galactoside protein sequence, each of them followed by a polyadenylation signal (Kassar-Duchossoy et al., 2004; Sambasivan et al., 2009; Tajbakhsh et al., 1996b). LoxP sites and frt sites on the transgene were designed to allow the use of this allele as a Cre-inducible stop-nlacZ reporter. For the Pax7$^{PN\text{-}H2BGFP}$ allele, the targeting vector contained a Pax7d cDNA sequence (accession NM_011039), a neomycin selection cassette and a fusion of histone H2B to green fluorescent protein (GFP) each of them followed by a polyadenylation signal. The H2BGFP fusion was made by PCR amplification of mouse H2B fused in frame at a Bgl II site to linker-EGFP construct (Shinin et al., 2009). Insertion of the floxed *Pax7d* cDNA cassette was aimed to generate a dual-purpose allele that would serve both as a conditional knock-out (cKO) as well as a Cre-inducible H2BGFP reporter. Owing to lack of expression of the *Pax7d* cassette, it could not be used as a cKO allele. Standard subcloning methods and recombineering (Liu et al., 2003) were used for vector construction. The targeting strategy for the generation of the *Pax7^{GPL}* and Pax7$^{PN\text{-}H2BGFP}$ lines is outlined in Fig. 2E. *Pax7^{GPL}* or Pax7$^{PN\text{-}H2BGFP}$ constructs were inserted into the *Pax7* locus via electroporation of CK35 (129sv) embryonic stem (ES) cells (Kassar-Duchossoy et al., 2004). Screening of correctly targeted ES cells were assessed by PCR and Southern blotting (Fig. S2A, B). Chimeric mice were bred to C57BL6/DBA2 mice. Germline transmission of the targeted alleles were assessed by PCR (see below). *Pax7^{GPL}* line was used to generate *Pax7^{nGFP}* and *Pax7^{nlacZ}* alleles by mating to either a ubiquitous Flippase (β-actin flippase; ActB:FLPe; (Rodriguez et al., 2000)) or Cre driver (PGK-Cre; (Lallemand et al., 1998)) lines, respectively.

Antibodies

Antibodies used in this study include Myosin heavy chain (rabbit polyclonal, kindly provided by G. Cossu, 1/750), β-galactosidase (rabbit polyclonal, kindly provided by O. Puijalon, 1/200), Myod (mouse monoclonal, 5.8.A, Dako, M3512, 1/50; rabbit polyclonal, Santa Cruz SC-704, 1/100), Laminin (rabbit polyclonal, Sigma 9393, 1/1000), GFP (chicken polyclonal, Abcam ab13970, 1/750 for sections, 1/2000 for myoblast cultures and single fibres), Pax7 (mouse monoclonal, DSHB, 1/10; rabbit polyclonal, Aviva systems biology ARP32742, 1/750), Myog (mouse monoclonal, F5D, DSHB, 1/50; rabbit polyclonal, Santa Cruz SC-576, 1/100), Cre (mouse monoclonal, Abcam ab24607, 1/1000; rabbit polyclonal, Novagen 69050, 1/3000).

Immunofluorescence

Tissue sections

Embryos were dissected in PBS, fixed in 4% paraformaldehyde in PBS for 1 h 30 min to 2 h at 4 °C and embedded in 7% gelatin and 15% sucrose for cryosectioning (12–16 μm). Dissected muscles were fixed in 2% paraformaldehyde, 0.5% Triton X100 in PBS and cryofrozen in isopentane bath (−30 °C) for sectioning (12–20 μm). Briefly, cryosections were allowed to dry for 5 min, blocked in PBS, 20% normal goat serum (GS), 0.5% Triton X100. Primary antibodies were diluted in the blocking solution and incubated overnight (ON) at 4 °C. After two 15 min washes in PBS, 0.1% Tween20, secondary antibodies (raised in goat, conjugated with Alexa 488 or 555 or 633 from Molecular Probes) were incubated in the blocking solution 1 h at RT together with 1μg/ml Hoechst to visualise nuclei. The sections were washed as above and mounted with coverslips in 75% glycerol Tris-buffered to pH 7. Images were acquired with a Zeiss Axioplan equipped with an Apotome and Axiovision software (Carl Zeiss, Jena, Germany, http://www.zeiss.com), or a Leica SPE confocal and Leica Application Suite (LAS) software. All images were assembled in Adobe Photoshop and Indesign (Adobe Systems, San Jose, CA, http://www.adobe.com). Some images were assembled as projections of successive confocal acquisitions. Optical sections (1–1.5 mm) were reconstructed using ImageJ (NIH).

Whole mount embryos

Embryos were harvested in PBS and screened for GFP expression under a Zeiss SteREO Discovery V20 microscope equipped with a Zeiss Axiocam MRc colour camera and the Axiovision software (Carl Zeiss, Jena, Germany, http://www.zeiss.com). Embryos were fixed overnight in 0.5% paraformaldehyde at 4 °C, and washed in PBS. The fixed embryos were permeabilized and blocked in 10% GS, 3% bovine serum albumin, 0.5% Triton X-100 and incubated subsequently in primary and secondary antibodies overnight in blocking solution. Images were acquired with the same Zeiss stereomicroscope.

Freshly isolated myoblasts

Tibialis anterior, masseter and extraoccular muscles were dissected and placed into cold DMEM. Muscles were then chopped with small scissors and put in a 15ml Falcon tube containing 10ml of DMEM (31966 Gibco®), 0.1% collagenase D (Roche 1088866), 0.25% trypsin (15090-046 Gibco®) at 37 °C under gentle agitation for 30 min. Digests were stored for 5 min at RT and the supernatants were collected in 5 ml of Fœtal Bovine Serum (Gibco®) on ice. Collagenase/trypsin solution was added to each tube and the incubation repeated 3 to 4 times till complete digestion of the muscle. The collected supernatants were pooled and filtered through a 70 μm cell strainer (BD Falcon). Cells were spun 15 min 515 rcf at 4 °C and the pellets resuspended in 1ml of culture media (20% FBS, 1% Penicillin–Streptomycin (15140 Gibco®), 2% Ultroser™ G (15950-017 Pall Biosepra) in 50:50 DMEM: F12 (31966 and 31765 Gibco®). Cells were plated on glass coverslips coated successively with 10 μg/ml poly-D-lysine (P6407 SIGMA) and matrigel (354234 BD Biosciences). Cells were allowed to attach to the coverslips in a 20% O_2 5% CO_2 37 °C incubator for 18 h. For immunostaining, cells were fixed in PBS, 4% PFA for 5 min at RT, washed with PBS and permeabilized with PBS, 0.5% Triton X-100 for 5 min. After three washes with PBS, cells were blocked with PBS, 20% GS 1h at RT. Primary antibodies were added to cells in PBS, 2% GS in PBS for 2–3 h at RT under gentle rocking. Cells were washed three times with PBS then incubated 1 h RT with Alexa-conjugated secondary antibodies (Molecular Probes® 1/1000) and 1 μg/ml Hoechst. Coverslips were mounted on glass slides with VECTASHIELD® Mounting Media. Images for quantification were acquired on a Leica SPE confocal and Leica Application Suite (LAS) software.

Isolated EDL fibres

Single fibres were isolated as described previously (Gayraud-Morel et al., 2007). Briefly, EDL muscles were dissected from adult mice (6–10 weeks old) and incubated for 1h DMEM 0.2% collagenase (C-0130, Sigma) at 37 °C. Following collagenase treatment, muscles were transfered to DMEM (31966 Gibco®) and fibres were mechanically dissociated by successive (<10) flushing using an eroded glass pasteur pipette. For time zero experiments, fibres were fixed for 5 min with PBS, 4% PFA at RT and subsequently washed 3 times in PBS. Otherwise, fibres were cultured in suspension in non-treated culture dishes in 20% FBS, 1% Penicillin–Streptomycin (15140 Gibco®), in 50:50 DMEM:F12 (31966 and 31765 Gibco® at 37 °C in 5% CO_2 20% O_2 for either 26 or 72 h. Myofibres were fixed in PBS, 4% PFA for 5 min as above.

Fixed myofibres were permeabilised in a solution of 20 mM HEPES, 300 mM sucrose, 50 mM NaCl, 3 mM $MgCl_2$ and 0.5% Triton X-100 (pH 7) at 4 °C for 15 min as described by Collins-Hooper et al. (2012). Fibres were washed in PBS 3 times. Non specific binding was blocked using the Mouse-On-Mouse Immunodetection Kit Vector® M.O.M.™ Kit as indicated by the manufacturer. Briefly, fibres were blocked on M.O.M blocking reagent for 1 h at RT. Mouse monoclonal anti-Cre antibody was added to fibres in M.O.M diluent solution with 0.05% Triton X-100 and incubated for 2 h at 4 °C plus 30 min at RT under gentle rocking. Fibres were washed three times with PBS and incubated with M.O.M biotinylated anti-mouse in diluent for 30 min at RT. After three PBS washes, anti-Myod, Pax7, Myog and or GFP polyclonal antibodies were added in PBS, 2% GS, 0.01% Triton X-100 o/n at 4 °C. The next day fibres were washed three times in PBS and incubated 1 h at RT in Cy3™-conjugated Streptavidin (Jackson ImmunoResearch 1/1000) to visualise mouse primary Cre antibody plus Alexa Fluor 488 or 633 goat-anti-rabbit and anti-chicken antibodies (Molecular Probes® 1/1000) in PBS, 2% GS, 0.01% Triton X100, 1 μg/ml Hoechst. After three washes in PBS fibres were mounted with VECTASHIELD® Mounting Media. Images were acquired on a Leica SPE confocal and Leica Application Suite (LAS) software. Images at time 0 h and 26 h represent a stack of two focal planes whereas images at time 72 h represent a stack of 8 focal planes.

X-gal staining and in situ hybridisation

Embryos were fixed briefly on 4% PFA for 40 min to 1 h depending on the embryonic day, washed with PBS and incubated overnight at 37 °C in standard X-gal staining solution (Tajbakhsh et al., 1997). *ISH* was performed as described (Kassar-Duchossoy et al., 2004; Tajbakhsh et al., 1997) with an anti-sense *Pax7* riboprobe.

Quantitative RT-PCR

Total RNA was extracted from cells isolated by FACS or isolated EDL and TA muscle fibres using the Qiagen RNAeasy Micro purification Kit. From the E12.5 embryos and E17.5 foetuses, limbs were dissected, digested in 0.2% trypsin or 0.1% Collagenase D (Roche) and 0.2% trypsin, respectively (Gayraud-Morel et al., 2007) and sorted based on GFP fluorescence using a FACSAria, BD and FACSDiva. Cells were directly sorted into lysis buffer for RNA preparation. From 400 to 600 ng of DNAse-treated (Roche) RNA, cDNA was prepared by random-primed reverse transcripion (SuperScript II, Invitrogen) and real-time PCR done using *power*SYBR Green Universal Mix or Taqman universal Master Mix (ABI Prism 7700 and StepOnePlus (Perkin-Elmer Applied Biosystems). GAPDH and TBP transcript levels were used for the normalisations of each target ($=\Delta CT$). At least 3 biological replicates were used for each condition and $2^{-\Delta CT}$ was plotted (Schmittgen and Livak, 2008). Custom primers were designed using the Primer3Plus online software (http://www.bioinformatics.nl/cgi-bin/primer3plus/primer3plus.cgi). Serial dilutions of total cDNA were used to calculate the amplification efficiency of each primer set according to the equation: $E=10\text{-}1/\text{slope}$. Primer dissociation experiments were performed to assure that no primer dimers or false amplicons would interfere with the results.

Statistics

The graphs were plotted and statistical analyses were performed using GraphPad Prism software. All data points are mean $\pm$ standard error of mean (error bars). Student *t*-tests were performed to calculate *p*-values of triplicate RT-q-PCR data. For comparing GFP^{Hi} versus GFP^{Lo} fractions of same samples, two-tailed, paired *t*-test was done. For comparing foetal versus embryonic samples two-tailed, unpaired *t*-tests were performed (*: $p<0.05$; **: $p<0.01$; ***: $p<0.001$).

Authors' contributions

R.S. and S.T. conceived the study. R.S., G.C., I.L.R. and S.T. participated in the design and wrote the manuscript. R.S., G.C. and I.L.R. performed the experiments and interpreted the results. R.S., S.T. and D.G. generated the *Pax7* knock-in mice. J.K. performed and interpreted some of the *in vitro* experiments. G.D. and C.C. provided technical support with histology and mice. Authors read and approved the final manuscript.

Acknowledgements and funding

We thank M. Capecchi, and M. Haldar for kindly providing $Mrf4^{Cre}$ mice. S.T. acknowledges support from the Institut Pasteur, Centre National de la Recherche Scientifique, Association Française contre les Myopathies (AFM), Agence Nationale de la Recherche (ANR-06-BLAN-0039), and the Fondation pour la Recherche Médicale.

Appendix A. Supporting information

Supplementary data associated with this article can be found in the online version at http://dx.doi.org/10.1016/j.ydbio.2013.04.018.

References

Armand, O., Boutineau, A.M., Mauger, A., Pautou, M.P., Kieny, M., 1983. Origin of satellite cells in avian skeletal muscles. Arch. Anat. Microsc. Morphol. Exp. 72, 163–181.

Beauchamp, J.R., Heslop, L., Yu, D.S., Tajbakhsh, S., Kelly, R.G., Wernig, A., Buckingham, M.E., Partridge, T.A., Zammit, P.S., 2000. Expression of CD34 and Myf5 defines the majority of quiescent adult skeletal muscle satellite cells. J. Cell Biol. 151, 1221–1234.

Berkes, C.A., Tapscott, S.J., 2005. MyoD and the transcriptional control of myogenesis. Semin. Cell Dev. Biol. 16, 585–595.

Biressi, S., Molinaro, M., Cossu, G., 2007a. Cellular heterogeneity during vertebrate skeletal muscle development. Dev. Biol. 308, 281–293.

Biressi, S., Tagliafico, E., Lamorte, G., Monteverde, S., Tenedini, E., Roncaglia, E., Ferrari, S., Cusella-De Angelis, M.G., Tajbakhsh, S., Cossu, G., 2007b. Intrinsic phenotypic diversity of embryonic and fetal myoblasts is revealed by genome-wide gene expression analysis on purified cells. Dev. Biol 304, 633–651.

Braun, T., Arnold, H.H., 1994. ES-cells carrying two inactivated myf-5 alleles form skeletal muscle cells: activation of an alternative myf-5-independent differentiation pathway. Dev. Biol. 164, 24–36.

Christ, B., Ordahl, C.P., 1995. Early stages of chick somite development. Anat. Embryol. 191, 381–396.

Collins-Hooper, H., Woolley, T.E., Dyson, L., Patel, A., Potter, P., Baker, R.E., Gaffney, E.A., Maini, P.K., Dash, P.R., Patel, K., 2012. Age-related changes in speed and mechanism of adult skeletal muscle stem cell migration. Stem Cells 30, 1182–1195.

Dellavalle, A., Maroli, G., Covarello, D., Azzoni, E., Innocenzi, A., Perani, L., Antonini, S., Sambasivan, R., Brunelli, S., Tajbakhsh, S., Cossu, G., 2011. Pericytes resident in postnatal skeletal muscle differentiate into muscle fibres and generate satellite cells. Nat. Commun. 2, 499.

Gayraud-Morel, B., Chretien, F., Flamant, P., Gomes, D., Zammit, P.S., Tajbakhsh, S., 2007. A role for the myogenic determination gene Myf5 in adult regenerative myogenesis. Dev. Biol 312, 13–28.

Gayraud-Morel, B., Chretien, F., Jory, A., Sambasivan, R., Negroni, E., Flamant, P., Soubigou, G., Coppee, J.Y., Di Santo, J., Cumano, A., Mouly, V., Tajbakhsh, S., 2012. Myf5 haploinsufficiency reveals distinct cell fate potentials for adult skeletal muscle stem cells. J Cell Sci. 125, 1738–1749.

Gensch, N., Borchardt, T., Schneider, A., Riethmacher, D., Braun, T., 2008. Different autonomous myogenic cell populations revealed by ablation of Myf5-expressing cells during mouse embryogenesis. Development 135, 1597–1604.

Goulding, M.D., Chalepakis, G., Deutsch, U., Erselius, J.R., Gruss, P., 1991. Pax-3, a novel murine DNA binding protein expressed during early neurogenesis. EMBO J. 10, 1135–1147.

Gros, J., Manceau, M., Thome, V., Marcelle, C., 2005. A common somitic origin for embryonic muscle progenitors and satellite cells. Nature 435, 954–958.

Haldar, M., Karan, G., Tvrdik, P., Capecchi, M.R., 2008. Two cell lineages, myf5 and myf5-independent, participate in mouse skeletal myogenesis. Dev. Cell 14, 437–445.

Harel, I., Nathan, E., Tirosh-Finkel, L., Zigdon, H., Guimaraes-Camboa, N., Evans, S.M., Tzahor, E., 2009. Distinct origins and genetic programs of head muscle satellite cells. Dev. Cell 16, 822–832.

Hasty, P., Bradley, A., Morris, J.H., Edmondson, D.G., Venuti, J.M., Olson, E.N., Klein, W.H., 1993. Muscle deficiency and neonatal death in mice with a targeted mutation in the myogenin gene. Nature 364, 501–506.

Hinterberger, T.J., Sassoon, D.A., Rhodes, S.J., Konieczny, S.F., 1991. Expression of the muscle regulatory factor MRF4 during somite and skeletal myofiber development. Dev. Biol. 147, 144–156.

Horst, D., Ustanina, S., Sergi, C., Mikuz, G., Juergens, H., Braun, T., Vorobyov, E., 2006. Comparative expression analysis of Pax3 and Pax7 during mouse myogenesis. Int. J. Dev. Biol. 50, 47–54.

Hutcheson, D.A., Zhao, J., Merrell, A., Haldar, M., Kardon, G., 2009. Embryonic and fetal limb myogenic cells are derived from developmentally distinct progenitors and have different requirements for beta-catenin. Genes Dev. 23, 997–1013.

Ivanova, A., Signore, M., Caro, N., Greene, N.D., Copp, A.J., Martinez-Barbera, J.P., 2005. In vivo genetic ablation by Cre-mediated expression of diphtheria toxin fragment A. Genesis 43, 129–135.

Kanisicak, O., Mendez, J.J., Yamamoto, S., Yamamoto, M., Goldhamer, D.J., 2009. Progenitors of skeletal muscle satellite cells express the muscle determination gene MyoD. Dev. Biol. 332, 131–141.

Kassar-Duchossoy, L., Gayraud-Morel, B., Gomès, D., Rocancourt, D., Buckingham, M., Shinin, V., Tajbakhsh, S., 2004. Mrf4 determines skeletal muscle identity in Myf5:Myod double-mutant mice. Nature 431, 466–471.

Kassar-Duchossoy, L., Giacone, E., Gayraud-Morel, B., Jory, A., Gomes, D., Tajbakhsh, S., 2005. Pax3/Pax7 mark a novel population of primitive myogenic cells during development. Genes Dev. 19, 1426–1431.

Keller, C., Arenkiel, B.R., Coffin, C.M., El-Bardeesy, N., DePinho, R.A., Capecchi, M.R., 2004a. Alveolar rhabdomyosarcomas in conditional Pax3:Fkhr mice: cooperativity of Ink4a/ARF and Trp53 loss of function. Genes Dev. 18, 2614–2626.

Keller, C., Hansen, M.S., Coffin, C.M., Capecchi, M.R., 2004b. Pax3:Fkhr interferes with embryonic Pax3 and Pax7 function: implications for alveolar rhabdomyosarcoma cell of origin. Genes Dev. 18, 2608–2613.

Kuang, S., Kuroda, K., Le Grand, F., Rudnicki, M.A., 2007. Asymmetric self-renewal and commitment of satellite stem cells in muscle. Cell 129, 999–1010.

Lallemand, Y., Luria, V., Haffner-Krausz, R., Lonai, P., 1998. Maternally expressed PGK-Cre transgene as a tool for early and uniform activation of the Cre site-specific recombinase. Transgenic Res. 7, 105–112.

Lepper, C., Conway, S.J., Fan, C.M., 2009. Adult satellite cells and embryonic muscle progenitors have distinct genetic requirements. Nature 460, 627–631.

Liu, P., Jenkins, N.A., Copeland, N.G., 2003. A highly efficient recombineering-based method for generating conditional knockout mutations. Genome Res. 13, 476–484.

Ma, Q., Zhou, B., Pu, W.T., 2008. Reassessment of Isl1 and Nkx2-5 cardiac fate maps using a Gata4-based reporter of Cre activity. Dev. Biol. 323, 98–104.
Mauro, A., 1961. Satellite cell of skeletal muscle fibers. J. Biophys. Biochem. Cytol. 9, 493–495.
Messina, G., Biressi, S., Monteverde, S., Magli, A., Cassano, M., Perani, L., Roncaglia, E., Tagliafico, E., Starnes, L., Campbell, C.E., Grossi, M., Goldhamer, D.J., Gronostajski, R.M., Cossu, G., 2010. Nfix regulates fetal-specific transcription in developing skeletal muscle. Cell 140, 554–566.
Mitchell, K.J., Pannerec, A., Cadot, B., Parlakian, A., Besson, V., Gomes, E.R., Marazzi, G., Sassoon, D.A., 2010. Identification and characterization of a non-satellite cell muscle resident progenitor during postnatal development. Nat. Cell Biol. 12, 257–266.
Mourikis, P., Gopalakrishnan, S., Sambasivan, R., Tajbakhsh, S., 2012a. Cell-autonomous Notch activity maintains the temporal specification potential of skeletal muscle stem cells. Development 139, 4536–4548.
Mourikis, P., Sambasivan, R., Castel, D., Rocheteau, P., Bizzarro, V., Tajbakhsh, S., 2012b. A critical requirement for notch signaling in maintenance of the quiescent skeletal muscle stem cell state. Stem Cells 30, 243–252.
Muzumdar, M.D., Tasic, B., Miyamichi, K., Li, L., Luo, L., 2007. A global double-fluorescent Cre reporter mouse. Genesis 45, 593–605.
Nabeshima, Y., Hanaoka, K., Hayasaka, M., Esumi, E., Li, S., Nonaka, I., Nabeshima, Y., 1993. Myogenin gene disruption results in perinatal lethality because of severe muscle defect. Nature 364, 532–535.
Novak, A., Guo, C., Yang, W., Nagy, A., Lobe, C.G., 2000. Z/EG, a double reporter mouse line that expresses enhanced green fluorescent protein upon Cre-mediated excision. Genesis 28, 147–155.
Rawls, A., Morris, J.H., Rudnicki, M., Braun, T., Arnold, H.H., Klein, W.H., Olson, E.N., 1995. Myogenin's functions do not overlap with those of MyoD or Myf-5 during mouse embryogenesis. Dev. Biol. 172, 37–50.
Rawls, A., Valdez, M.R., Zhang, W., Richardson, J., Klein, W.H., Olson, E.N., 1998. Overlapping functions of the myogenic bHLH genes MRF4 and MyoD revealed in double mutant mice. Development 125, 2349–2358.
Relaix, F., Rocancourt, D., Mansouri, A., Buckingham, M., 2005. A Pax3/Pax7-dependent population of skeletal muscle progenitor cells. Nature 435, 948–953.
Relaix, F., Zammit, P.S., 2012. Satellite cells are essential for skeletal muscle regeneration: the cell on the edge returns centre stage. Development 139, 2845–2856.
Rocheteau, P., Gayraud-Morel, B., Siegl-Cachedenier, I., Blasco, M.A., Tajbakhsh, S., 2012. A subpopulation of adult skeletal muscle stem cells retains all template DNA strands after cell division. Cell 148, 112–125.
Rodriguez, C.I., Buchholz, F., Galloway, J., Sequerra, R., Kasper, J., Ayala, R., Stewart, A.F., Dymecki, S.M., 2000. High-efficiency deleter mice show that FLPe is an alternative to Cre-loxP. Nat. Genet. 25, 139–140.
Rudnicki, M.A., Schneglesberg, P.N.J., Stead, R.H., Braun, T., Arnold, H.-H., Jaenisch, R., 1993. MyoD or myf-5 is required for the formation of skeletal muscle. Cell 75, 1351–1359.
Sambasivan, R., Gayraud-Morel, B., Dumas, G., Cimper, C., Paisant, S., Kelly, R.G., Tajbakhsh, S., 2009. Distinct regulatory cascades govern extraocular and pharyngeal arch muscle progenitor cell fates. Dev. Cell 16, 810–821.
Sambasivan, R., Kuratani, S., Tajbakhsh, S., 2011. An eye on the head: the development and evolution of craniofacial muscles. Development 138, 2401–2415.
Sambasivan, R., Tajbakhsh, S., 2007. Skeletal muscle stem cell birth and properties. Semin. Cell Dev. Biol 18, 870–882.
Schmittgen, T.D., Livak, K.J., 2008. Analyzing real-time PCR data by the comparative C(T) method. Nat. Protocols 3, 1101–1108.
Seale, P., Sabourin, L.A., Girgis-Gabardo, A., Mansouri, A., Gruss, P., Rudnicki, M.A., 2000. Pax7 is required for the specification of myogenic satellite cells. Cell 102, 777–786.
Shinin, V., Gayraud-Morel, B., Tajbakhsh, S., 2009. Template DNA-strand co-segregation and asymmetric cell division in skeletal muscle stem cells. Methods Mol. Biol. 482, 295–317.
Soriano, P., 1999. Generalized lacZ expression with the ROSA26 Cre reporter strain. Nat. Genet. 21, 70–71.
Stanley, E.G., Biben, C., Elefanty, A., Barnett, L., Koentgen, F., Robb, L., Harvey, R.P., 2002. Efficient Cre-mediated deletion in cardiac progenitor cells conferred by a 3'UTR-ires-Cre allele of the homeobox gene Nkx2.5. Int. J. Dev. Biol. 46, 431–439.
Tajbakhsh, S., 2009. Skeletal muscle stem cells in developmental versus regenerative myogenesis. J. Intern. Med. 266, 372–389.
Tajbakhsh, S., Bober, E., Babinet, C., Pournin, S., Arnold, H., Buckingham, M., 1996b. Gene targeting the myf-5 locus with LacZ reveals expression of this myogenic factor in mature skeletal muscle fibres as well as early embryonic muscle. Dev. Dyn. 206, 291–300.
Tajbakhsh, S., Buckingham, M., 2000. The birth of muscle progenitor cells in the mouse: spatiotemporal considerations. Curr. Top. Dev. Biol. 48, 225–268.
Tajbakhsh, S., Rocancourt, D., Buckingham, M., 1996a. Muscle progenitor cells failing to respond to positional cues adopt non-myogenic fates in myf-5 null mice. Nature 384, 266–270.
Tajbakhsh, S., Rocancourt, D., Cossu, G., Buckingham, M., 1997. Redefining the genetic hierarchies controlling skeletal myogenesis: Pax-3 and Myf-5 act upstream of MyoD. Cell 89, 127–138.
Vooijs, M., Jonkers, J., Berns, A., 2001. A highly efficient ligand-regulated Cre recombinase mouse line shows that LoxP recombination is position dependent. EMBO Rep. 2, 292–297.
Wu, S., Wu, Y., Capecchi, M.R., 2006. Motoneurons and oligodendrocytes are sequentially generated from neural stem cells but do not appear to share common lineage-restricted progenitors in vivo. Development 133, 581–590.
Zhang, W., Behringer, R.R., Olson, E.N., 1995. Inactivation of the myogenic bHLH MRF4 gene results in up-regulation of myogenin and rib anomalies. Genes Dev. 9, 1388–1399.